Marshall University
Marshall Digital Scholar

Theses, Dissertations and Capstones

2000

Feature extraction in geobiophysical modeling of mining activity impacting Dewey Lake, Kentucky

Sean K. Litteral

Follow this and additional works at: https://mds.marshall.edu/etd

Part of the Geology Commons

Recommended Citation
Litteral, Sean K., "Feature extraction in geobiophysical modeling of mining activity impacting Dewey Lake, Kentucky" (2000). *Theses, Dissertations and Capstones*. 1714.
https://mds.marshall.edu/etd/1714

This Thesis is brought to you for free and open access by Marshall Digital Scholar. It has been accepted for inclusion in Theses, Dissertations and Capstones by an authorized administrator of Marshall Digital Scholar. For more information, please contact zhangj@marshall.edu, beachgr@marshall.edu.

FEATURE EXTRACTION IN GEOBIOPHYSICAL MODELING OF MINING ACTIVITY IMPACTING DEWEY LAKE, KENTUCKY

A Thesis

Submitted to the Graduate College of

Marshall University

Huntington West Virginia

In Partial Fulfillment

of the Requirement for the Degree

Master of Physical Science

In

Geobiophysical Modeling

By

Sean K. Litteral

August, 2000

This thesis was accepted on August 8 2000.
Month Day Year

as meeting the research requirements for the master's degree.

Ralph E. Oberly

Professor Ralph E. Oberly, Ph. D.

Dewey D. Sanderson

Professor Dewey Sanderson, Ph. D.

Professor James O. Brumfield, Ph. D.
Advisor
Coordinator of Graduate Physical Science Program

Leonard J. Deutsch

Leonard J. Deutsch, Ph. D.
Dean of Graduate School

ACKNOWLEDGMENTS

I would like to thank the committee members for their support and friendship. The chairman of the committee Dr. Jim Brumfield, were it not for his help, encouragement and patience, this project would have been most difficult. Another member of my committee deserving special thanks was Dr. Dewey Sanderson. His special attention to detail and computer knowledge along with helpful suggestions made this thesis possible. I would also like to thank Dr. Ralph Oberly for his support throughout the project.

In particular, thanks go to the special effort of Dr. George P. Kincaid with the U.S. Army Corps of Engineers, Huntington District, who provided the digital images for the study. Without his desire for the pursuit of knowledge, this project would not have been possible. Others who deserve special credits and thanks include Dr. Protip Ghosh, Professor, Marshall University; without his early mentoring and advice a master's degree would never have been attainable. I would also like to thank him for his guidance and friendship throughout the degree program. Thanks to Dr.Richard Bonnett, Professor, Marshall University for his support throughout my studies at Marshall University. Thanks to Richard Petit, Radiation Safety Specialist, Marshall University for his help and expertise with computer support.

I would like to gratefully thank my son, Matthew Litteral, and parents, Norman and Charlene Litteral, for their love and support, who suffered the physical effects of added financial burdens along with lost time and have not swayed in their emotional supported of my efforts. Finally, I would like to thank ER Mapper and the U.S. Army Corps of Engineers for grants involved with this project.

TABLE OF CONTENTS

FIGURE LIST

LIST OF TABLES

ABSTRACT

Surface coal mining activity has effects on watershed and lake morphology within the Appalachian Mountains that continue to be problematic. A watershed's natural dynamic balance has been subject to the influence of various natural and anthropogenic parameters such as mining sediment transport, wind, wave effects and currents. Many techniques have been developed to improve image processing in geobiophysical modeling, which can assist scientists, government officials, and industry personal with decisions affecting environmental concerns. One of the more advanced techniques involves 3D visualization and geobiophysical modeling. This process was used in combining remotely sensed digital aerial imagery with Digital Elevation Models (DEM). This assisted the analyst by creating a much more accurate geobiophysical model of the earth's surface. This was accomplished as a result of simulating the moderate to high topographic relief found within the mountainous terrain environments of the Appalachian Mountain's coalfields. Feature extraction was improved as well as visual interpretation.

The research objective was to develop and evaluate new techniques for combining 3D Models with feature extraction processes and thereby creating more accurate thematic information classification maps. Improved techniques result from radiometric corrections, increased resolution, and data enhancement from the DEM's. The method used incorporated the advantages of several software packages (ER Mapper, Surfer, and ArcView). These packages provide different image processing and geographic information system capability. Clusters were identified in ER Mapper with classification techniques for feature extraction. This was the process used to identify clusters of similar data in the frequency domain of an

image that correlate to different vegetation, urban and/or rural areas. The research results show a substantial improvement in feature extraction and 3D-geobiophysical modeling.

Chapter One

INTRODUCTION

1.1 OVERVIEW

The mountains have been largely ignored within the remote sensing community due to the complexity of the interaction contained by mountainous terrain's geology, hydrology, climate and biological processes. Bloemer et al, (1996) defined the problem as:

> "Remote sensing for cartography in mountainous regions has been largely ignored because process and change often occur on a much smaller spatial scale representing higher spatial frequencies. Higher spatial frequency variability require higher resolution spatial analysis over similar spectral bands to extract comparable features found on flood and coastal plains."

Remotely sensed data has been used in studies to evaluate surface mining in the eastern United States. This is in response to the Federal Surface Mine Control and Reclamation Act (Public Law 95-87 enacted in 1977). It advanced the prevention of environmental degradation and corrected problems caused in the past by previous mining (Irons et. al, 1980). Problems that led to this action were insufficient mine reclamation, that left unsightly landscape, ruined productive land, increased susceptibility to flooding and created water quality problems. Other environmental troubles with surface mining included erosion, gullying, acid-mine drainage and increased sediment load as a result of abandoned and un-reclaimed mined lands (Parks et. al. 1987).

In reaction to this law, government agencies and mine operators were required to monitor reclamation practices which created a need for inventorying mined acreage.

These requirements caused a problem with regulatory agencies of providing cost effective monitoring of surface mines, so the investigation into the utility of remote sensing for surface mine monitoring got underway.

Severe land disruption and degradation was one of the most obvious impacts of surface mining. Mapping the aerial extent and location was important in formulating strategies for reclamation once mining has ceased. A study by Chase and Pettyjohn (1973) was probably the earliest to report the utility of ERTS-1 MSS data in mapping land disruptions due to strip mining in east-central Ohio. The study concluded that strip mines could be easily identified by satellite imagery without the aid of aerial photos or maps. Standing water could also be delineated in either spectral band 6 or 7. Signifying the importance of land disruption, the study stressed monitoring of lands was perhaps most important from an ecological viewpoint. It was, however, not possible to identify reclamation work done near the site as it was barely detectable on the ERTS-1 imagery. Similar results in delineation of surface mine workings using ERTS-1 imagery were also reported by Wier et al. (1973). However, another similar parallel study by Alexander et al. (1973) to monitor and map strip mine activity near Pennsylvania along the west branch of the Susquehanna River succeeded not only in isolating areas affected by mining, but also sub-classifications of the strip mined areas such as trenched areas, backfill, acid-mine drainage, new stripping and partially vegetated zones. Areas affected by acid mine drainage could also be located on the ERTS-1 imagery by identifying areas of dead or dying vegetation. The use of unsupervised cluster analysis on the digital data has provided excellent results when applied with a discriminate function such as a principal component or canonical analysis (Brumfield et. al. 1983). Carr et. al. (1983), however, observed that unsupervised algorithms have maximum utility in classifying images where limited field information was available for accurate location of training sites or where a large number of spectral classes were present. Where numerous scenes were to be classified with few terrain classes of interest and where field information was available to assist training, a supervised classification was most suitable in mined-lands applications (Carr et al, 1983).

Areas under active mining or areas that have been abandoned can present special problems in digital classification because a considerable amount of confusion was generated due to the similarity in spectral signatures of mined surfaces and other cover types such as bare agricultural fields, barren or rocky surfaces, etc. A number of workers have found the use of conventional classification algorithms unsuitable for producing acceptable classifications for land disrupted by mining. A number of alternative schemes for identifying land impacted by mining operations were developed. Anderson and Schuber (1976) used band ratioing (MSS band 5 and MSS band 7) successfully to delineate, map and inventory the effects of strip mining in the upper Potomac and Georges Creek basins of Maryland and West Virginia. The study was further extended by Anderson et al. (1977) to inventory effects of strip mining in a 1540-km^2 area in western Maryland. Anderson et al. (1977) used two methods to produce classification maps. The first of these methods was a supervised parallelepiped algorithm applied to the 4-band MSS data after selecting training areas. Variation in spectral radiance among the 4-band signatures for various strip-mining surfaces revealed such classification operationally ineffective in monitoring studies. There were considerable differences in signature within a mined area and, therefore, the training statistics could not be extrapolated to other parts of the study area. It was observed, however, that band ratioing prior to classification considerably minimized the effects of environmental and sensor conditions on feature signature extraction. Band ratioing, by minimizing these environmental effects, provided extendible signatures for features that could be used in other parts of the study area. In all, twelve ratios (combinations of the 4 MSS bands i.e. green, red, and near infrared) were individually compared with results of aerial photographs to derive a standard error in classification. The ratio of band 5/band 6 (red/near infrared) was found to have the least error and was subsequently used. The average accuracy in preparing a surface mine inventory was determined to be greater than 92 percent after comparing with aerial photographs of the area. The utility of band ratioing (MSS-5/MSS-6) in measuring total area disturbed by mining was further authenticated by Irons et al. (1980). They attributed the utility of MSS-5/MSS-6 ratio to the distinct contrast between partially re-vegetated surface mine spoil and dense vegetation in the surrounding areas.

Solomon et al. (1979) developed a tree classifier to discriminate surface mine activity using Landsat-MSS digital data. In previous studies it had been apparent that signatures obtained from the four bands of Landsat-MSS data had large variations for different types of strip mining surfaces. In the development of the tree classifier, ratioing different combinations of the original four bands generated five channels of data, in addition to the four MSS bands. Signatures of various cover types were trained using cluster analysis on a small subset of the data. The best four channels, i.e., the channels that maximize repeatability, were determined and the tree classifier developed using this information. A number of land cover classes and sub-classes which include forest, agriculture, scrubland, urban, water and mining activity (rough spoil, smoothed, and partially vegetated) could be discriminated over the study area using the classifier. The classification output also aided in accurate estimation of areas disturbed by mining. The classifier was, however, unable to determine cover conditions over narrow contour mines.

More recent studies in this area have emphasized a variety of techniques. In 1980 Irons et al.and Spisz and Dooley compared satellite and airborne multispectral scanner data, along with color infrared (CIR) aerial photography, for surface mine assessment. Brumfield et al. (1983) used canonical analysis to compare transformed datasets with unsupervised clustering for surface mine mapping in Logan Co., West Virginia, and found improvements of up to 15% in overall classification accuracy

Parks et al. (1987) also compared the utility of MSS, TM and simulated SPOT data for studying surface mining activity over central Pennsylvania. The classification scheme used for comparison was modified from Anderson (1971) to specifically address land covers associated with mining. Findings of this study suggested that MSS data was useful for large area monitoring but unsuitable for identification of level 3 categories of the classification scheme. Collins et al. (1991) emphasized simulated spot and TM data accurately identified level 3 categories that were comparable to each other with TM having an advantage of higher spectral resolution over SPOT. Harding (1988), while studying sand and gravel pits, has observed no significant difference in classification accuracy between TM and SPOT data.

1.11 MINE REVEGETATION AND RECLAMATION MONITORING

Abandoned mine sites represent stressed and nutritionally deficient environments for plant growth. Mularz (1979) highlighted some of the special problems encountered in mine reclamation. Usually a considerable amount of money and effort was required in reclaiming abandoned mine lands. Successful monitoring and reclamation programs, therefore, relied heavily on periodic monitoring of planted areas such that the plant growth and vigor could be regularly estimated and corrective action taken if required. Remote sensing techniques have been used extensively for monitoring reclaimed mine sites (Bauer 1973, Gilbertson 1973, Kirby 1974, Jaques 1977, Anderson and Tanner 1978, Bloemer et al 1981, Brumbaugh 1979, Johannsen et al. 1979, and Green and Buschur 1980).

In one of the earlier studies, Carrel et al. (1978) used both manual and computer based techniques to interpret aerial photographs for monitoring reclamation activity at a strip mine in Missouri. The manual method involved first preparing a transparent overlay clearly demarcating the total area covered by the aerial photographs. In similar fashion, then, transparent overlays of total vegetation, woody vegetation and water bodies in the strip mine area were also prepared interpreting low altitude aerial photographs. Areas of bare soil or sparse vegetation were then determined by subtracting the above overlays from the outline overlay representing total area covered by the mine. The second method involved applying computer classification algorithms to a digitized version of the same aerial photographs. The accuracy of the computer classification was determined by registering the classified image print out to the aerial photograph and putting an identically numbered equal sized grids on both of them for comparison. Classification accuracy was observed to generally be high for bare soil and water categories but relatively poor for the vegetation category. Misclassifications occurred mainly because the dark shale material was confused with surrounding vegetation and water. Both vegetation and water appeared darker than bare soil on positive prints.

Mroczynski and Weismiller (1982) have used color aerial infrared photography for evaluating reclaimed and non-reclaimed land in an area covering 18,783 km^2 across 20 counties in southwestern Indiana. Manual photointerpretation techniques were used to interpret 1:30,000 scale color infrared photographs. These photos were enlargements of 1: 120,000 high altitude positive transparencies acquired by NASA in 1971. Interpretation procedures were designed to treat each county as an independent unit and township areas within counties were examined for possible derelict sites. Maps identifying derelict mined lands across the 20 counties were prepared from these interpretations for use by the Indiana Division of Reclamation for their inventorying and planning procedures. Over 4700 hectares of abandoned mined lands and 800 hectares of possible affected water area were identified through this study (Mroczynski and Weismiller 1982). Of the total area identified as derelict, 62 percent was barren spoil, 15 percent was courser refuse or gob piles, 14 percent probable affected water bodies and 9 percent was covered by slurry ponds. Subsequent field verifications revealed that 64 percent of the possible derelict sites were under different landcover categories as a number of the sites had been reclaimed since the acquisition of the aerial photographs in 1971. Of the existing derelict land, estimation for accuracy revealed a very high percentage of individual and overall (98 percent) accuracy estimations (Mroczynski and Weismiller, 1982).

In a more recent study by Halverson (1988), high altitude aerial photography has been used to monitor and assess success of reforestation on four mines in the state of

Kentucky. Color infrared transparencies at a nominal scale of 1:58 000 were used for this study. Out of these four mine sites, one mine site resisted repeated reforestation attempts. Two of the other mine sites were reforested except for some areas and one remaining mine site was bare and yet to be reforested. Manual interpretation of the transparencies revealed that very dark color areas appeared on the three reclaimed sites were the areas where reforestation problem had been encountered in the past. Similar dark areas appearing on the site where reforestation was to start were identified as potentially problematic areas. Although Halverson (1988), did not isolate the cause for the dark color on the aerial photographs, the author did suggest that changes in soil moisture (possible increase on non-vegetated site), organic matter in soil (possible increase due to coal wasted) and iron oxide (possible increased due to the presence of iron pyrites) could be responsible for the very dark color on each mine site that was associated with reclamation problems.

Satellite data has been used for monitoring reclamation work on abandoned mine sites. In one of the studies by Legg, 1986, Landsat Thematic Mapper data was used to assess vegetation vigor at reclamation sites at the Butterwell opencast coal mine and the Druridge Bay area of the United Kingdom. Vegetation vigor studies were carried out on the reclaimed lands using band ratioing. A composite image depicting the sum of the ratios of near infrared for eight co-registered scenes used in the study was produced. Lighter tones on the composite image indicated higher ratio values and thus unstressed vegetation. Comparisons with similar vegetation on unmined lands revealed that vigor was, on average, lower on reclaimed lands as compared to unmined control of the surrounding areas. This difference in plant vigor was most observable during the growing season in spring when the grass on reclaimed land appeared to lag behind the grass on the unmined land in terms of growth.

1.12 WATER POLLUTION ASSESSMENT

Surface and underground mining have caused water pollution resulting in serious environmental problems. Among other pollutants, acid mine drainage, heavy metal contamination and high concentrations of suspended and dissolved solids have caused specific concern. Acid mine drainage was produced when water came into contact with pyritic material (iron sulfides) and oxygen in coal mines. Weathering of this pyritic material eventually produced sulfuric acid, which not only lowered water pH, but also increased solubility of metal ions such as iron, aluminum, manganese and zinc (Kenny and McCauley 1982). Water contaminated by acid mine drainage was usually characterized by a reddish-yellow color due to ferric oxide precipitates and was extremely detrimental to most aquatic flora and fauna.

Digital satellite data has been used in the past to monitor pollution levels of selected parameters in water bodies (Lathrop and Lillesand 1986, 1988, Lillesand et. al, 1987). Alfoldi (1982) gives a review of some of the issues involved in satellite remote sensing of selected water quality parameters. Similar references to studies conducted for the assessment of water quality over surface coal mine sites using remotely sensed data are few. Repic et al. (1991) pointed out that the relatively poor spatial resolution of satellite data was one of the major constraints. Most of the water bodies created by strip mines are small or narrow and the poor spatial resolution of satellite data was not suitable for water quality analysis.

Kenny and McCauley (1982) used aerial photography to study stream quality degradation due to mining and to locate point sources responsible for pollution of streams. This study confined itself to the Cherry Creek basin area in Cherokee County, Kansas, which had a number of abandoned surface mines. Color and color infrared photography at 1:10 000 scale were used in this study. Twenty-six sampling stations were established on the ground covering the stream network in this study area and water samples collected from these sites were analyzed for parameters like stream flow, pH, specific conductivity, dissolved iron, dissolved manganese, dissolved aluminum, dissolved zinc, dissolved sulphate and suspended sediment. Acid mine drainage detected from the color photographs as red-yellow precipitate of ferric oxide on streambed, waste piles and drainage. The study found that the two major drainage areas in the study site had different levels and types of stream water degradation. These differences were mainly attributed to dissimilarities in surface contours, status of reclaimed lands, nature of coal mines and the age of the mines. Aerial photographs revealed that one of these drainage areas, the eastern part of the basin under study, was well vegetated. This vegetation prevented soil erosion and, as a result, water in strip pits appeared clear on the imagery. Surface water quality measurements revealed the water in these pits to be very acidic. When these sites were inspected, it was found that water from a number of these strip pits drained into the ground through shafts and sinkholes and that the surface was hydraulically connected to the deep mines. Highly contaminated acidic water then found its way to the surface through openings such as fractures, drillholes, bedding plains, air shafts etc., creating serious pollution problems. These seepages were visible on the aerial photographs. The other drainage area of the western part of the basin was devoid of seeps and sinkholes. No direct connection between the surface and deep underground mines was observed. Due to application of lime on spoil banks in this area and due to lack of substantial vegetation, water in this area was observed to be alkaline with higher suspended solid loads.

More recently, Repic et al. (1991) have used narrow band multi-spectral video imagery to study acidity and metal contamination (iron) at two water bodes at a surface coal mine in Clay County, Indiana. Video imagery was acquired in the yellow-green (0.543 to 0.552 micro meter), red (0.644 to 0.656 micro meter) and near-infrared ranges (0.815 to 0.827 micro meter) from an altitude of 2400 m using narrow band filters on cameras sensitive in the visible and near-infrared regions. Water samples were collected from 14 locations over the water bodies and analyzed for pH and iron content. These sample locations were then identified on the video imagery and at each location; the mean digital value of a 3 by 3 window of pixels centered at the identified sample location was calculated to avoid mislocation errors. This was done for all 14 water samples and each band. Digital values, at each sample location, were correlated with the pH and iron content at that location. Correlation results showed the yellow-green band to be positively correlated (significant at 0.05 level) with pH values, possibly because increased iron in solution was caused by increased acidity. Repic et al. (1991) suggested that these high correlations of the yellow-green band with pH and iron were due to the fact that the increased iron content in the water gave it a yellow-orange color to which the yellow-green band was more sensitive, as compared to the red or the near-infrared bands. The study concluded that the yellow-green band of the video imagery was most sensitive to pH and the iron ion content of surface mine water. This band can be used to monitor iron contamination and acidity in coal strip mine drainage area.

1.13 REMOTE SENSING AND GEOGRAPHICAL INFORMATION SYSTEMS

Barr (1981) has suggested that combining geological, geographical and Landsat derived information in the form of a natural resource database holds great potential for monitoring mining areas. This concept, known as a Geographical Information System (GIS), has become an indispensable tool for environmental monitoring and planning. Since monitoring involved periodic assessment of cover conditions in an area and remote sensing was a practical and often used way to monitor, the input of classified images into a GIS, which also held other thematic map layers of the area, greatly enhanced its functionality and use. A number of issues, however, needed to be addressed in order to couple remotely sensed data with a GIS (Jensen, 1986). In the context of environmental monitoring of mining areas, there was very little literature on GIS applications and its interface with remotely sensed data. A recent study however illustrated the tremendous potential of interfacing remotely-sensed data and GIS for environmental monitoring. Oberg et al. (1982), have monitored environmental impacts of oil shale mining in northeastern Estonia using Landsat-MSS of 1986 and SPOT XS, band 2 data and have used the results of this analysis in a geographical information system. The resultant image revealed that the opencast mine area had expanded by approximately 13.01 km^2 between 1986 and 1991. A supervised classification using the maximum likelihood classifier was also performed on the data and the classified image was vectorized and transferred to the ARC/INFO system. Thematic attributed such as planned areas for future mining activities were available as digitized ARC/INFO coverage from the Estonia Nature Management Scientific Information Center (ENMSIC) GIS databases (Oberg et al.1982). A polygon overlay of the two coverages highlighted aerial extents of different landuse/cover classes, such as forests, wetlands, and peat area, for example, would be directly impacted by future mining operations in the region. The utilization of remotely sensed data in this manner not only provided geographically relevant information for various environmental planning programs but also ensured that the interpreted data is available for analysis at a later point in time.

Previous works have been concerned mainly with the ability to accurately identify and measure the aerial extent of surface mines. Evaluation of the utility of remote sensing varied from study-to-study depending on the data sources, analysis techniques, and geographic areas under investigation (Bloemer et al. 81, 82). Landsat data had been well established as accurate in its ability to identify and measure surface mines. Thus, the current trend was toward a mixture of data sets with multisensor and multitemporal information. Data transformations with PCA or Canonical analysis were utilized for feature extraction in mining activities (Brumfield, et al. 1983).

1.2 STATEMENT OF PURPOSE

The demand for coal as energy had increased. This created a conflict over mining practices and maintaining a quality environment. Currently, surface mining had disturbed millions of acres across the United States. At present, 60% of the nation's coal comes from surface mining practices. Inadequate reclamation had left unattractive landscape, destroyed previously productive land, and caused air and water pollution (Irons et al, 1980). The influence of surface coal mining activity on lake morphology and ecology within the Appalachian Mountains proved to be inadequately understood. Lake morphology had a natural dynamic balance being subject to the influence of various natural parameters such as sediment transport, wind, wave effects and currents. Short and long-term lake morphology changes were of great importance to regulatory and monitoring agencies. This study evaluated and modeled the relationship between coal mining activity and its anthropogenic influence on lake morphology, due to a heavy-suspended load, acid mine drainage, and stressed vegetation originating mainly from improper mining practices. The color of the lake area affected by mining activity was vastly different from the normal watercolor within Dewey Lake Watershed. Taking into account the properties of the water quality and the local sediment transport, qualitative and relative quantitative information about some parameters related to lake morphology may be recovered from aerial images. Remotely sensed digital aerial imagery served as the data for feature extraction in pattern recognition for geobiophysical modeling within the project study area.

"The conditions of the mountains with regard to hydrology, vegetation, lithologic outcrops, and their effect upon regional and, ultimately, global cycles impacting forests are linked" (Comins and Noble, 1985). The results of this study aided in the understanding and development of new techniques to study surface coal mining activities in mountainous environments, that affect the delicate ecosystems within the Appalachian Mountains.

The objective was to create a geobiophysical model with new techniques for a combination of 3-D Models with feature extraction. The geobiophysical model integrated the biosphere, geosphere and hydrosphere with an emphasis on mountainous terrain affected by surface mine activity. Brumfield (1990) gave the first definition for a geobiophysical modeling system. He defines it as:

> "... an integrated series of analytical modeling procedures. It provides spatial and statistical scientists, engineers and multi-disciplinary resource planners with a framework for integrating many different types of information decision making processes. Through these procedures, the volume of geobiophysical data (physical, biological, environmental, and socio-economic information pertaining to the biosphere, geosphere, hydrosphere and atmosphere), can be stored, managed, manipulated, analyzed, modeled and displayed."

Figure 1.1 was a schematic diagram showing the data and processing components for the

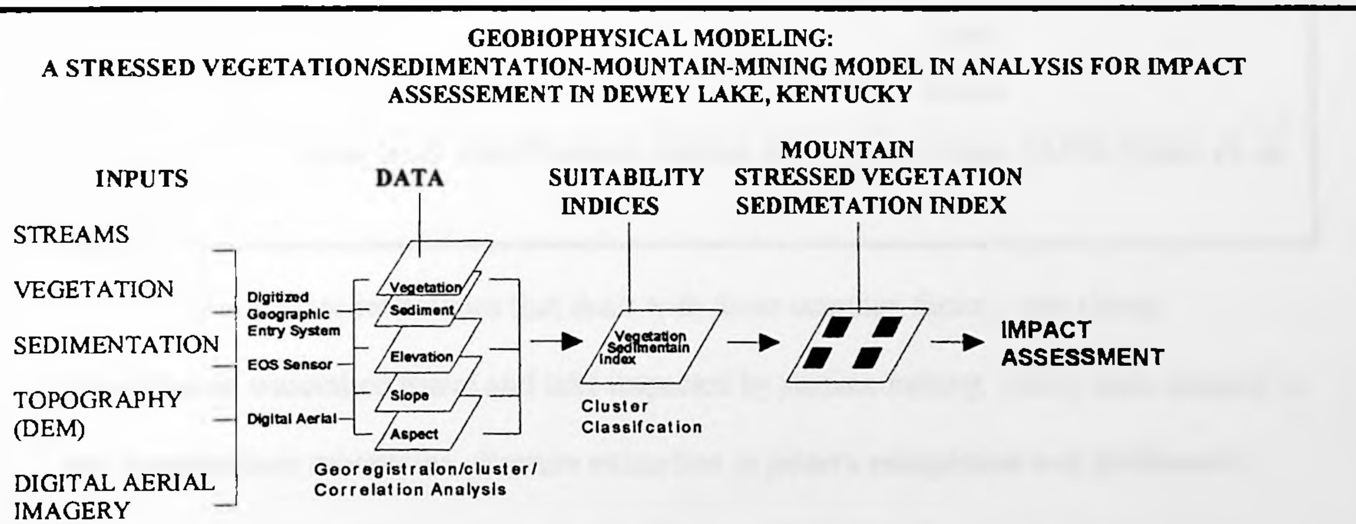

Figure 1.1. Diagram showing data processing component of a geobiophysical model.

geobiophysical model created for this study. The classification scheme used in this study was modified after Irons et al. (1980). This was a three level classification scheme that classifies detailed mine categories (Table 1.1) and had great potential for monitoring surface mine activity. Therefore, this was modified to include certain categories of environmental factors specifically designed to be classified within this study.

Level I	Level II	Level III
Agriculture	Pasture	
Forest	Deciduous	Deciduous
		Fall foilage
	Conifer	Conifer
		Stressed vegetation
Water		Suspended sediment load
Surface Mines	Bare mine soil	
	< 20 per cent vegetation	
	Bare soil mine soil	Ungraded
	Revegetated mine soil	Grass/trees
		Grass
		Roads

Table 1.1 A three level classification scheme for surface mines (After Parks et al. 1987).

To illustrate techniques that dealt with these complex factors, this thesis investigated watershed forest and lake impacted by surface mining, which were located in the Appalachian mountains. Feature extraction in pattern recognition was performed with multivariate associations by discrimination with PCA and analysis of variance/covariance on a high order spatial resolution or instantaneous field of view, of less than 1.0 m IFOV, for selected spectral bands. The resulting data were used for feature extraction affecting pattern recognition in physiognomy of species, identification of forest associations with physical environmental parameters. Sampling variability was evaluated by feature extraction in pattern recognition and geobiophysical modeling with analysis of variance/covariance (Mills, et al, 1963, Bloemer and Brumfield, et at, 1996).

Chapter Two

METHODS AND TECHNIQUES

A broad spectrum of spatial frequencies occurs in nature. In mountainous terrain these spatial frequencies represents numerous difficulties from a remote sensing perspective in that processes and change often occur on a much smaller spatial scale than typically observed on large plains. Higher spatial frequency variability requires higher spatial resolution and spatial analysis over similar spectral bands to extract comparable features (Brumfield, et. al., 1983; Bloemer, et al., 1996; Gervin, et al., 1996). An image data collection system was chosen with a 1 meter IFOV that can resolve the higher spatial frequencies in mountainous terrain. The methodologies employed in this research involved vegetation classification, production of near infrared color imagery, and 3D-visualization digital aerial imagery, datasets georectification and registration and 3-D geobiophysical modeling utilizing software systems such as ER Mapper, Surfer, and Arc-View.

2.1 SITE DESCRIPTION

The eastern Kentucky coalfield covered the eastern end of the state, stretching from the Appalachian Mountains westward across the Cumberland Plateau to the Pottsville Escarpment (Fig 2.1). The area was heavily forested and characterized by rolling topography with moderate relief. Geologically, the area was underlain by horizontal to gently dipping sedimentary strata of the Alleghany Group formed during the Pennsylvanian geologic period. Extensive portions have been disturbed by mountaintop-removal and contour mining. The general area had active mining and reclaimed locations

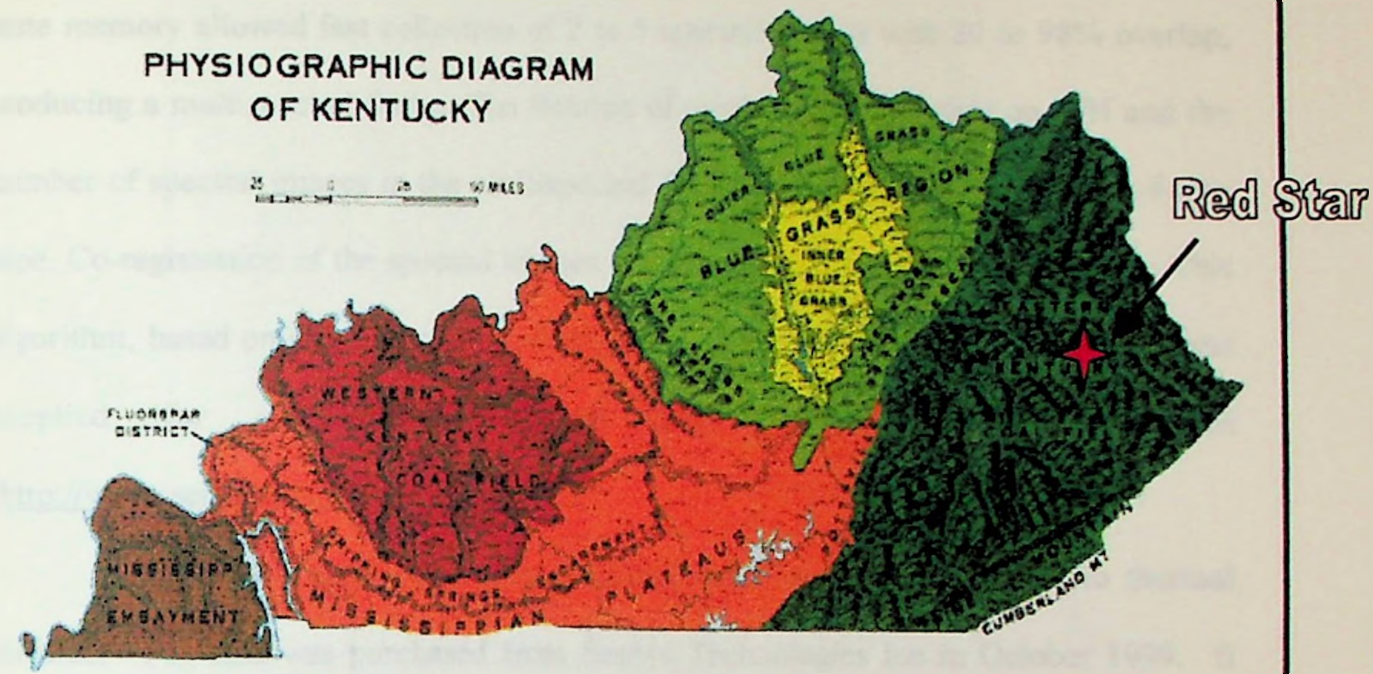

Figure 2.1. Location map for Dewey Lake. The red star indicates location of Dewey Lake. Modified from the Kentucky Atlas and Gazette.

making it an excellent study location. Situated within this environment was Jenny Wiley State Resort Park complete with 1,100-acre Dewey Lake. Located in Floyd County, it comprises 7,353 acres. The Lake was named for a brave pioneer woman who survived Indian capture in the area. The US Army Corps of Engineers leased this area to the state of Kentucky. Dewey Lake watershed, located in the Cumberland Plateau region of the state, had elevations ranging from 580 to 2320 feet above sea level. Environmental problems such as green-area damage, erosion, acid mine drainage and increased sediment loads in local streams and in Dewey Lake have resulted from coal mining activity.

2.2 DATA SOURCES AND INSTRUMENTATION

The AA497 Airborne Multispectral Digital Camera (AMDC) was a two-dimensional framing machine with 2000 pixels along in each onthogonal axis. Spectral images were created with optical filters on a movable wheel. Fast data transfer to solid-state memory allowed fast collection of 2 to 5 spectral images with 80 to 98% overlap, producing a multispectral frame. The fraction of overlap was dependent on V/H and the number of spectral images in the multispectral frame. The frame was recorded to 8-mm tape. Co-registration of the spectral images was done with a re-sampling algorithm. This algorithm, based on a two-dimensional projective transform and a flat earth model, was supplied for use in a ground data processing system reference (http://www.sensystech.com, 2000).

The data contained six bands of information, ranging from visible to thermal infrared. The data was purchased from Sensys Technologies Inc in October 1999. It received nominal correction for velocity to height (V/H) ratio and scan distortion from the company, but did not receive corrections for yaw errors. Due to considerable terrain relief geometric displacements were noted within the imagery. Rectification and Digital Elevation Models were used to correct these problems. All of the data were collected on 1 October 1999. All of the low altitude lines were flown between 11:00 a.m. and 2:00 p.m. local time. There was a total of 3 flight lines for this project labeled dl-2, dl-3, and dl-4 (fig 2.2). They were flown at a compass orientation of north-south, with 1-meter pixel resolution covering the mining area.

2.3 FIELD DATA COLLECTION

Dewey Lake was visited for ground based measurements. These measurements were specifically designed to test the accuracy of the classified clusters gathered from the digital aerial imagery. Seven sites were chosen to be tested for pH, temperature, and dissolved metals. The sites were then photographed with a Nikon Cool Pix 990 digital

Figure 2.2. Image created in ArcView 3.1 to show flight line coverage and orientation.

camera and vegetation type and condition were recorded. The pH was tested and recorded at each site. The surface water temperature was then recorded with an Atkins Infrared Thermometer Series 396K. The water was collected and taken back to the lab to be analyzed for dissolved metal content using an ICP Emission Spectrometer Model Liberty 110. This information was then entered into ArcView where a database was created. The photographs of the sites were then hot linked to complete the database.

2.4 IMPORTATION PROCEDURE

All data received was in ERDAS Imagine format. In order to utilize the data, ER Mapper's import utility was employed, by selecting with the track ball mouse on the **Utilities** menu, a dropdown list appeared (fig 2.3) with highlight on **Import Image formats;** this opened up another dropdown list. By selecting the **Import** module for

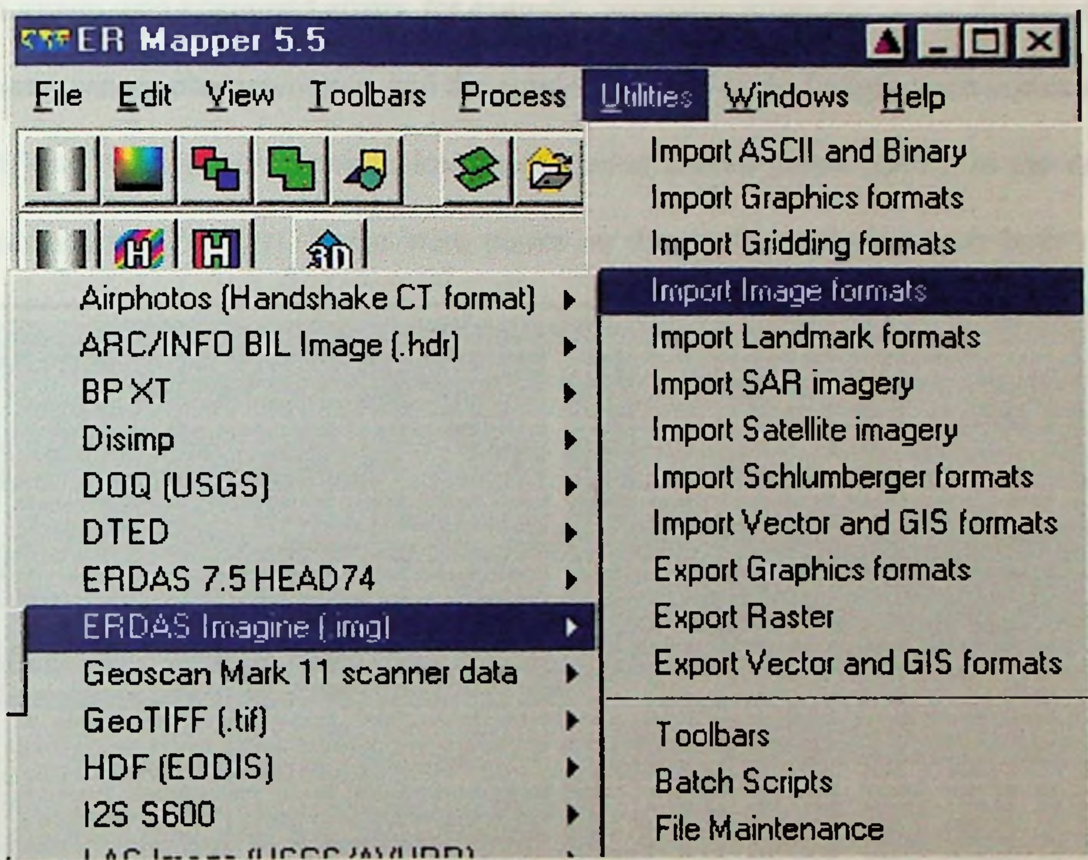

Figure 2.3. Picture showing locations of import dialog for ERDAS Imagine format using ER Mapper 5.5.

ERDAS Imagine (.img), the **Import dialog** box for the ERDAS Imagine format was opened. To import the complete dataset, the Input path name and Output path name were selected followed by selecting OK. Everything else was left to the default setting. This made it easier to adjust and be used for correct map projections later.

2.5 RECTIFICATION PROCEDURE

There are two important reasons why the data needed to be rectified. One was to mosaic it to another dataset and the second was to reference it to a geo-coordinate system. This allowed comparison of datasets by overlaying two or more images that are in the same coordinate system projection. Georeferencing was important because the digital aerial image data contained errors, for example, geometric errors due to the motion of the scanners, sensor characteristics, and the curvature of the earth. Images were corrected by identifying corresponding points, known as ground control points (GCP), in the dataset and on a map (Fig 2.4). These were points on the earth's surface where both image

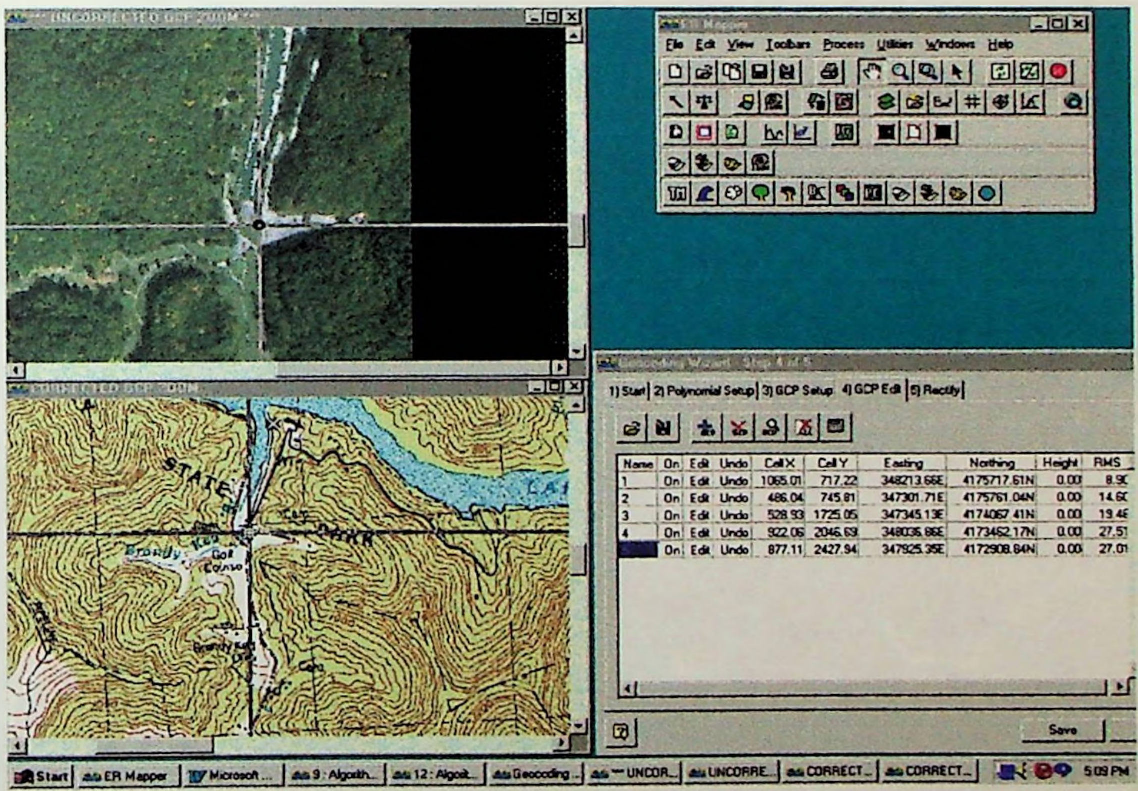

Figure 2.4. A location of ground control points, taken at a street intersection using ER Mapper 5.5

coordinates and map coordinates were identified. They were used in the rectification process to transform the geometry of an image so that each pixel corresponded to a position in a real world coordinate system. These control points were used to mathematically modify by 'rubber sheeting' the entire image. Geo-rectification or warping the data was stretching or compressing it to align with a real world map grid or coordinate system.

Each raw aerial image file was geocoded to a map projection. The image was referenced to a specific coordinate system and the position of any point in the image was related to a point on the Earth's surface. A 7.5 minute USGS topographic quad (1:24.000), projected in Kentucky State Plane South, NAD 83, US survey with feet as units was applied. These were downloaded from www.state.ky.us/ agencies/ finance/ depts/ ogis/ new_web/ data/ content.htm in the format of digital raster graphics (DRG) (See Fig 2.5). The DRG files were then imported into ArcView (ESRI, 1991-1999) where pixel

Figure 2.5. A Digital Raster Graphics (DRG) of Dewey Lake imported into ER Mapper 6.1.

size could be determined. This step was necessary because ER Mapper does not support (DRG) formats. In ArcView the file was opened up as a Tagged Image File Format (tiff) file under the **Add Theme** module, with the Data source type set to Image Data Source. The **View** menu **Properties** was selected in order to establish the correct map units and projection. In the **View Properties** table the Map Units of feet were selected and the Distance Units were set to meters. Selecting the **Projection** module set the projection. A new table was opened called **Projection Properties**. The Category was set to State Plane – 1983 and the Type was set to Kentucky, South. This made it possible to enlarge the image and determine pixel size by using the measuring tool. This process determined a pixel size of 2.6 meters for the DRG.

2.6 CREATED TIFF FILES

The tiff file was opened in ER Mapper and saved as a new ER Mapper dataset. The **Geocoding Wizard** available in version 6.1 makes this a simple procedure. Selecting the **Geocoding Button** on the main menu, opened the **Geocoding Wizard** window. The name of the new dataset just created was entered, followed by selecting the **Known point registration** option (Fig 2.6). Next, tab 2, the **Coordinate System Setup** was selected. This was information such as Datum, Projection, Coordinate Type and Units entered on the menu (Fig 2.6). The final tab, **Registration Point Edit**, was the information about pixel size and the Easting and Northing of the top left corner cell. This was determined previously in ArcView and entered to complete the (Fig 2.6). This became the dataset to be used as a reference map projection for the raw remotely sensed imagery.

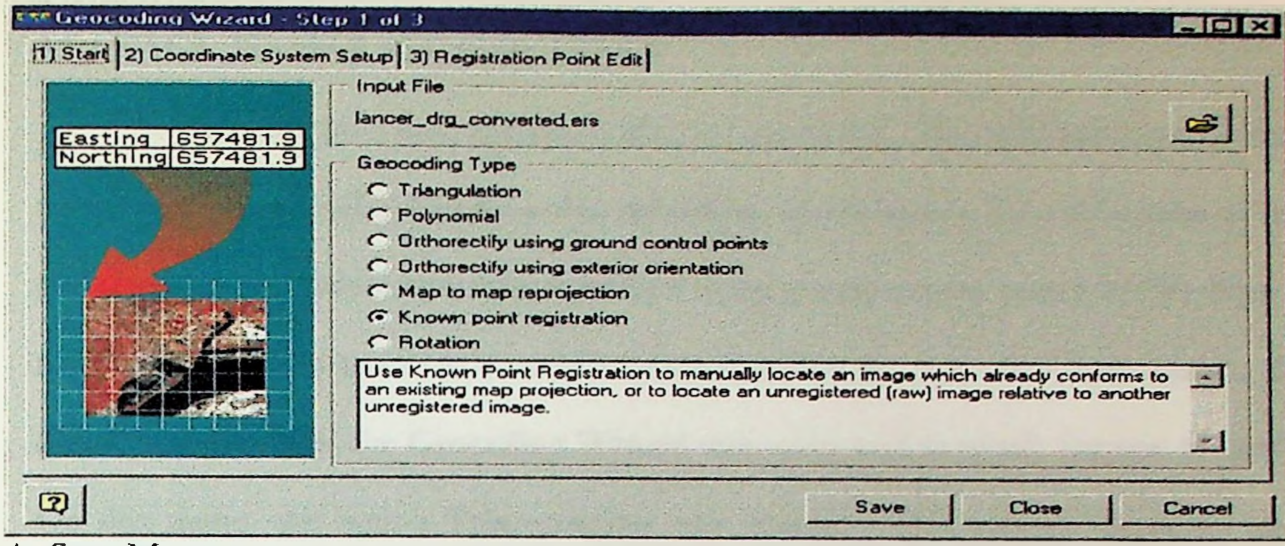

A. Start Menu.

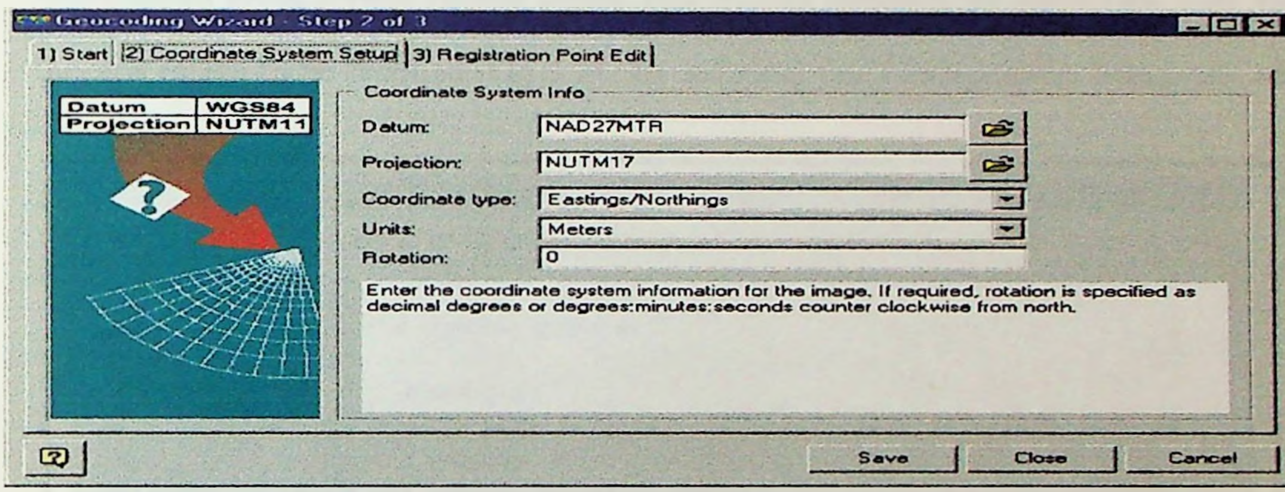

B. Coordinate System Menu.

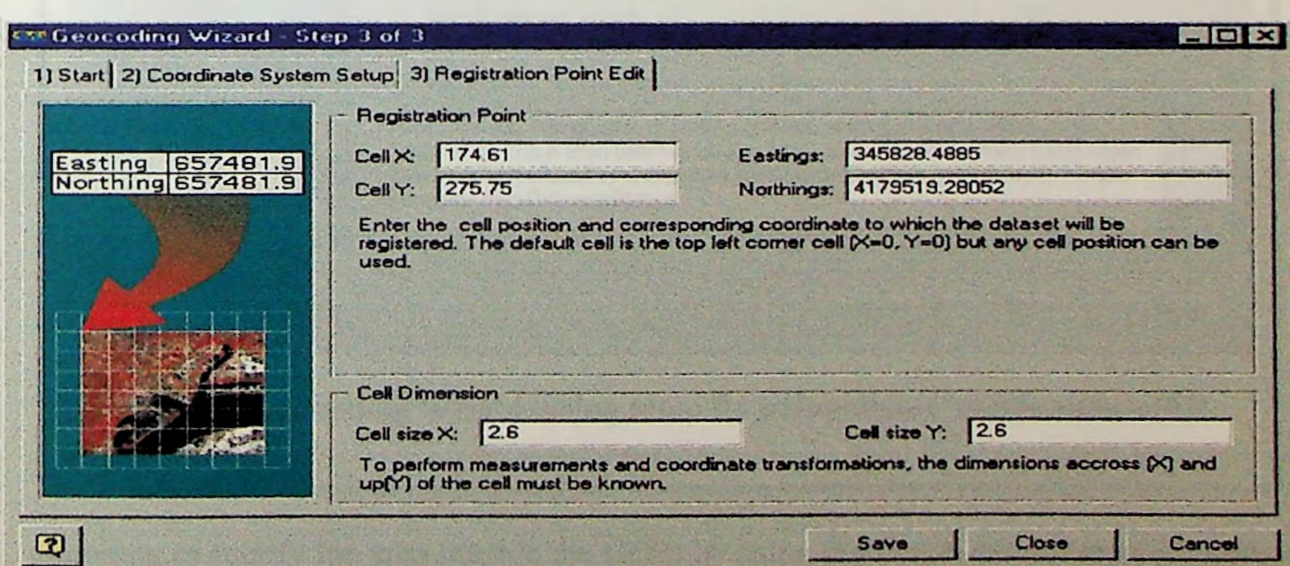

C. Registration Point Edit.

Figure 2.6. Menus for the Geocoding Wizard in ER Mapper 6.1.

2.7 IMAGE TO MAP RECTIFICATION

ER Mapper provided several rectification operations. The rectification performed in this section was called **Known point operation**. In this section the rectification of the raw imagery to a datum and map projection using ground control points (GCP) from a map was employed to create a rectified dataset within the new coordinate space. To accomplish this task, the **Geocoding Wizard** was again used to rectify the raw imagery. On this menu, the option **Triangulation** was selected. This was an image to map rectification using ground control points, followed by choosing the Input File. This was the raw image to be rectified (Fig 2.7). By selecting the **Triangulation Setup** tab, and

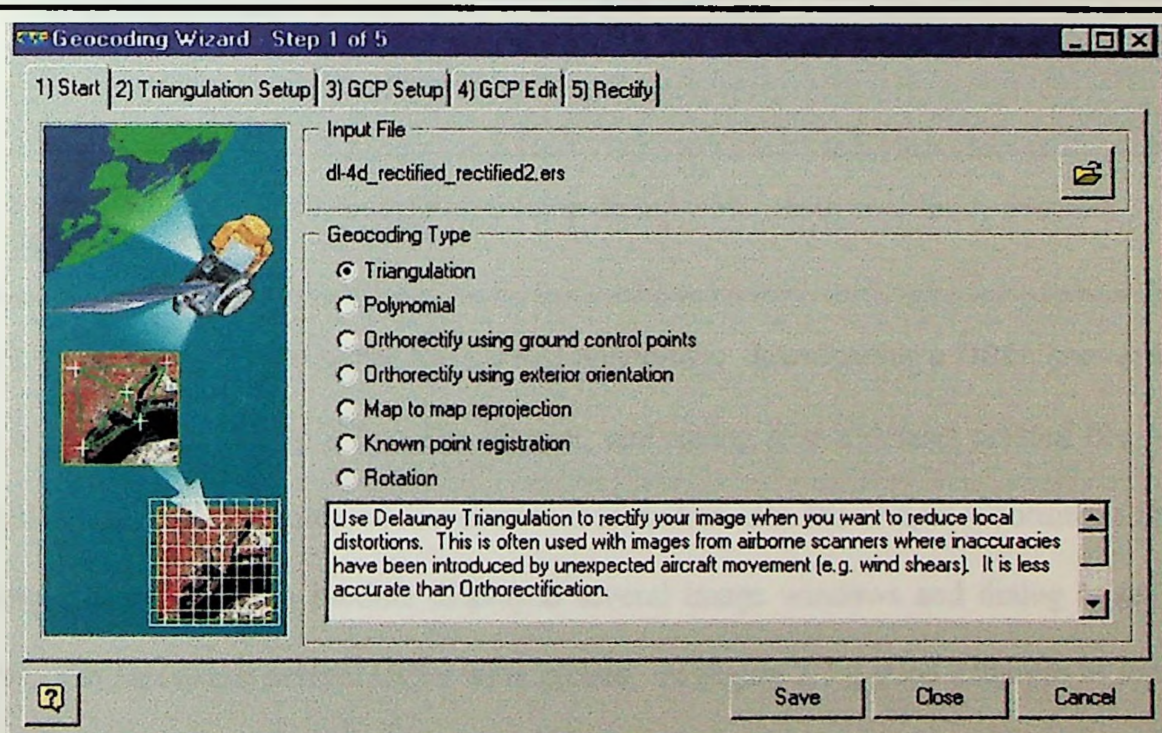

Figure 2.7. Geocoding Wizard dialog setup for triangulation rectification in ER Mapper 6.1.

choosing to rectify the area outside the GCPs by using the first order polynomial method, ER Mapper rectified the whole image rather than just the area on the map that was within the GCPs on the image. The third tab was selected bringing up the **GCP Setup** dialog (Fig 2.8). Next, the option, **Geocoded image, vectors or algorithm**, was selected. This

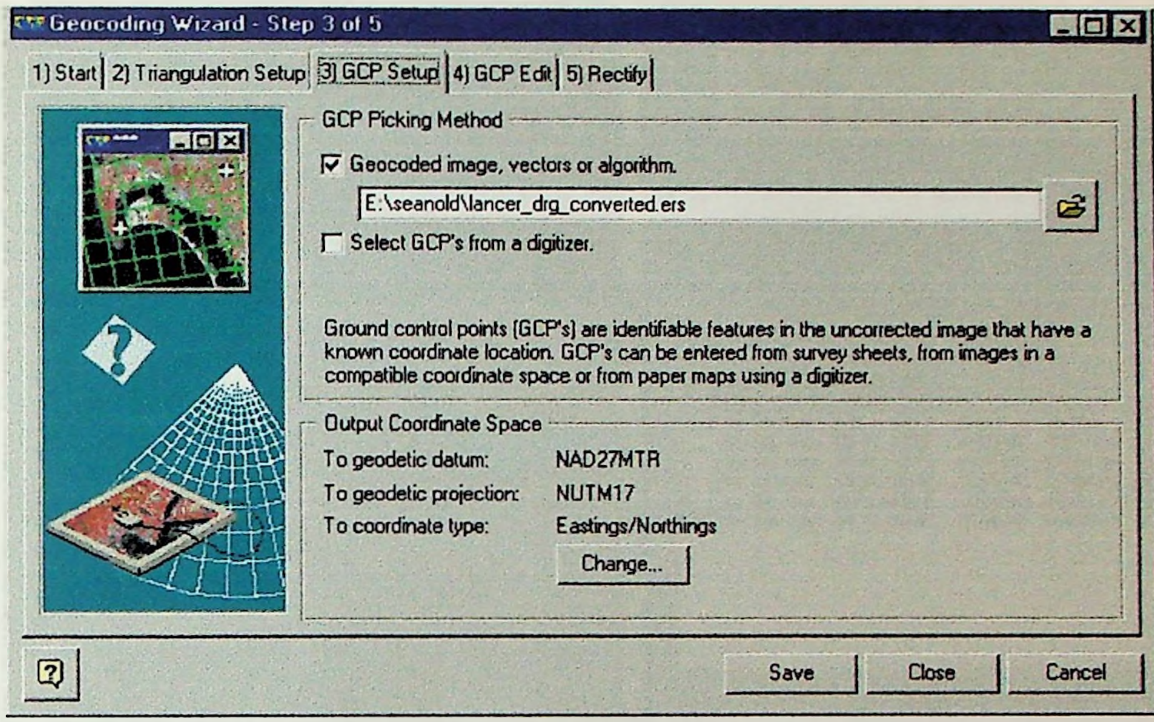

Figure 2.8. Ground Control Point Setup dialog with output coordinate space in ERMapper 6.1.

was followed by: entering the file created previously; downloading a DRG; converting it to a tiff file; importing it into ER Mapper, and saving it as a dataset created file. This option automatically entered the correct information into the Output Coordinate Space. Next, the **GCP Setup** module displayed several image windows and dialog boxes (Fig 2.9). On this menu several GCPs were picked. In Figure 2.7 a good example of locating GCPs was chosen on the raw uncorrected image and the control image was identified. Locations were chosen from clearly identifiable points on both the raw image and the control image. Fifteen control points were widely distributed across the image to provide a more stable solution. A constraint of the rural environment provided a maximum of 15 GCPs, which were selected for each image rectified. To complete the procedure, the

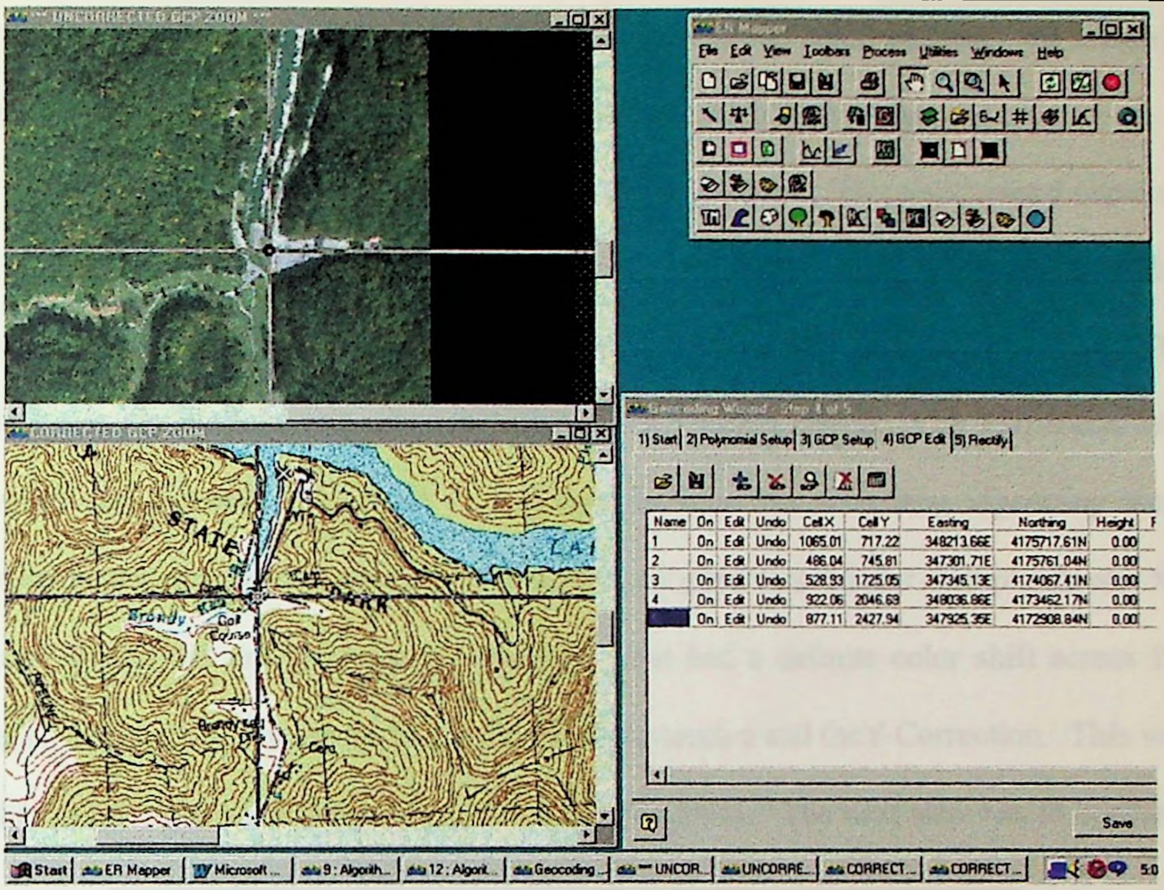

Figure 2.9. Display showing the raw uncorrected image with the corrected image. Also displayed is the Geocoding Wizard's GCPs screen. This screen lets you add and remove GCPs in ER Mapper 6.1.

Rectified module was selected. ER Mapper processed the rectification and geocoding of the corrected image. Automatically, the raw image was displayed and referenced to any other geocoded image. Thus, the other geocoded images were mosaicked together to produce an aerial image mosaic.

2.8 RADIOMETRIC CORRECTIONS

Once each aerial image was geocoded, it was radiometrically corrected by color and intensity. Color balancing corrected the tendency for the edges of an image to be bluer than the center of the image because they were further from the nadir. Intensity balancing corrected for changes in intensity in the aerial photograph from the center to the edges resulting from the thickness of the lenses in the aerial camera. To create a seamless mosaic image, these parameters were corrected in each image.

The linear brightness shift created a "roll off" problem. The edge toward one side of the image was darker, called vignetting. Within ER Mapper two basic formulas existed for correcting vignetting. These are located in the **Formula Editor** dialog. The **Edit Formula** module was selected within the Algorithm dialog. The File menu was selected and opened. The built in template formulas for correcting vignetting were located in the mosaic directory. The first formula used was 'Linear Ramp'. It was for images which did not have a clear 'hot spot', but had a definite color shift across the image. The variables were set to 0.3 for the X Correction and theY Correction. This was within the normal value range from -0.3 to 0.3 (fig 2.91). The next step was to combine

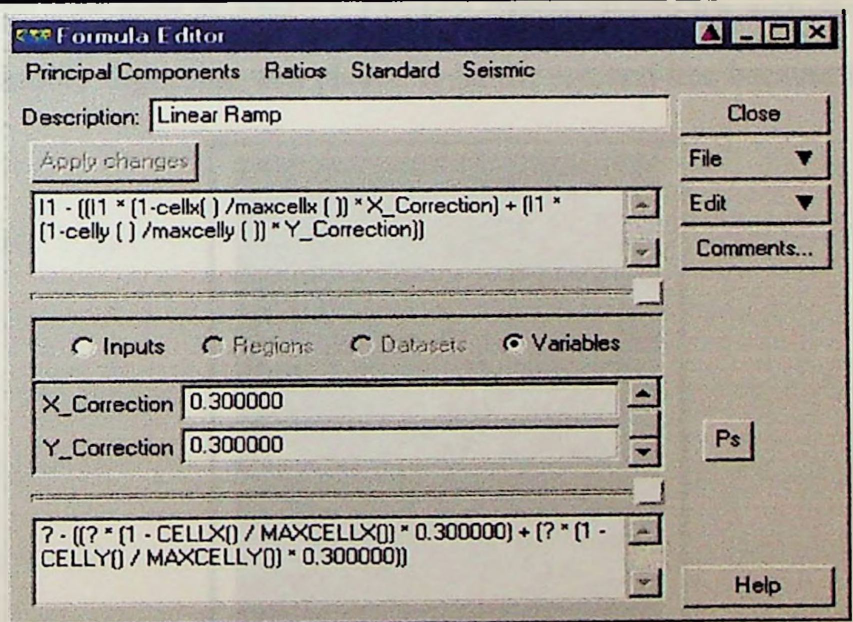

Figure 2.91. Formula Editor showing the Linear Ramp formula with X and Y corrections in ER Mapper 5.5.

two formulas using the "and" command. The next formula applied was intended to create an intensity or radiometric roll off correction from the identified center of the 'Hot Spot'. For this formula, the X center and Y center of the 'hot spots' were identified using the cell coordinate window. 0.3 was selected as the X and Y correction values to remove the color shifts. A failure occurred when trying to combine the formulas with the "and" command. This caused the screen to turn black. This was corrected by applying the formula and saving it as a new dataset, then applying the second formula. Once the images have been rectified, geocoded, and balanced they were ready to mosaic.

2.9 MOSAIC PROCEDURE

Mosaicking combined smaller images in order to generate a composite view of a larger area. ER Mapper was unique in that its algorithm concept includes features such as automatic data mosaicking. In order to assure seamless mosaics, a hidden stitch line was created. This was the portion of the digital aerial image to be shown. ER Mapper's annotation tool was used to define a polygon region around the area to be shown (Fig 2.92). The middle flight line was picked to be the stitched line because it had the most

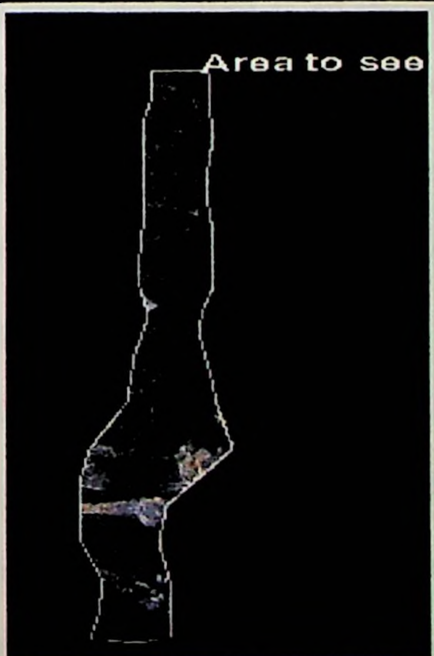

Figure 2.92. Image showing the creation of a hidden stitch line in ER Mapper 6.1.

overlap. A hidden stitch line eliminated the need to create a stitch line in the adjacent images. After defining the polygon, it was given the name "Area to see". Next the balancing formula was edited for each layer (Red, Green, Blue) to read: IF INREGION('Area to see') THEN <balancing formula> ELSE NULL(Fig 2.93). This masked all the area outside of the polygon. Within ER Mapper, mosaicking was automatic. Adding the other digital aerial imagery to the mosaic was accomplished by selecting the **Add New Surface** module on the Algorithm dialog that created a new surface layer. Another image could be added to the mosaic. If Ok was selected, this would apply the dataset to all the surface layers. Care must be taken to select "Apply this layer only option" located on the **Raster Dataset** module. This single process was applied to insert all images into the mosaic.

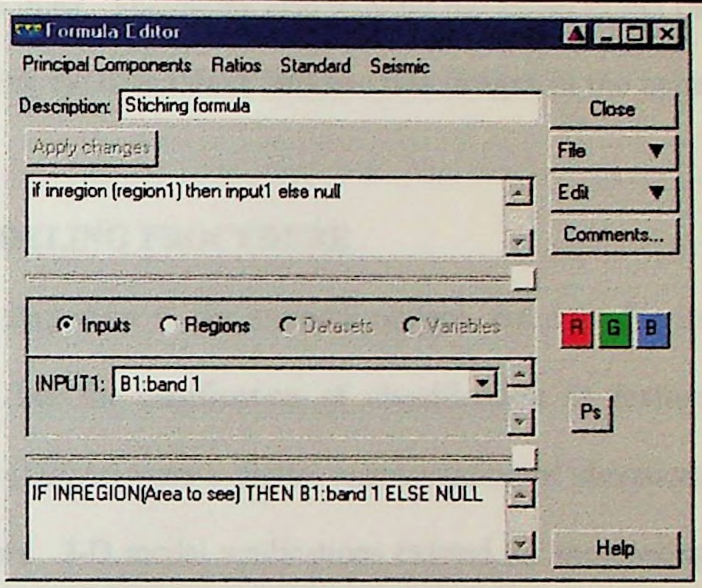

Figure 2.93. Display demonstrating the formula to create a stitch line.

After the images were mosaicked, further balancing was possible utilizing histogram matching. Histogram matching was a process that modified the transform lines for several datasets, which forced the output histograms to match the histogram of a reference dataset. Utilizing the standard technique to balance brightness across the mosaic, minimized image joining (mosaic) and made them appear to be one image. This was accomplished by selecting the **Edit Transform Limits** module in the Algorithm dialog. Selecting the **Histogram match** option for all layers and color completed the histogram match.

The **Feathering** option was used to increase the quality of the mosaic. Feathering was the process of blending the data values in areas where two datsets overlap so there was gradual transition from one to the other. Feathering also reduced the visual effect of seams. Feathering worked by averaging the data values between two images in the zone where there was overlap.

2.10 THREE-DIMENSIONAL MODELING PROCEDURE

3-demensional modeling was important to the research project, not only for its improvement in visual observation, but for clarification of classification in feature extraction. Digital Elevation Models (DEMs) were a digital representation of elevation, organized as a regular grid of numbers. 3-D model applications existed for monitoring surface water flow and evaluating elevation disturbances due to surface mine activity and urban development. DEMs were created and mosiacked into the finished product. The spacing between grid elements represents the interval between samples. The DEMs used were 30-meter grid spacings, meaning one elevation contour was sampled every 30 meters. The numerical value in each grid element represented the elevation at that point. The number was a floating point, to ensure that small variations in elevation can be recorded accurately.

These DEMs data files were produced by the U.S. Geological Survey (USGS) as part of the National Mapping Program and were available under the Download Data option from USGS. This was accomplished by selecting "Us Geo Data for selected geographic data in 7.5-minute" which was included in the large scale category. The

DEM data for the 7.5-minute units corresponded to the USGS 1:24,000 and 1:25,000 scale topographic quadrangle map series for all of the United States and its territories. Each 7.5-minute DEM was based on 30- by 30-meter data spacing with the Universal Transverse Mercator (UTM) projection. Each 7.5- by 7.5-minute block provided the same coverage as the standard USGS 7.5-minute map series (http://rmmcweb.cr.usgs.gov/elevation/, 2000).

The DEM Data files were downloaded and translated from Spatial Data Transfer Standard (SDTS) into DEM files. The American National Standards Institute's (ANSI) approved Spatial Data Transfer Standard (SDTS) was a mechanism for archiving and transferring of spatial data, including metadata, between dissimilar computer systems. The SDTS specified exchange constructs, such as format, structure, and content, for spatially referenced vector and raster, including gridded, data. The program used to translate the SDTS DEM files was SDTS2DEM.C created by Sol Katz, version .012. The program dumped SDTS DEM modules to a data file, which reconstructed the original dem source file. This was obtained from a website called Geocommunity located at www.geocomm.com. It utilized a DOS based format using Microsoft C. After downloading the program, it was uncompressed and opened. Trial and error instructions, used in the instructions, gave the first four character of the base file name (1234xxxx.ddf) then gave the output file without the .DEM extension. The first thing entered had to be the four character base (1234), followed by selecting return then by again entering 1234 then return again. The final step was to enter the cell id. This was the character in the 7th and 8th position of the filename, usually a L0 or l0. Care was taken here to enter zero (0) instead of Letter O. The files were transferred into .DEM file extensions, which were compatible with ER Mapper.

A problem discovered with the DEMs was that edges did not match correctly (Fig 2.94 a. and b.) in ER Mapper. This was corrected by importing and merging the SDTS DEMs in Surfer (See Table 2.1 below). Figure 2.95 displayed corrected DEMs.

Merging SDTS DEM in Surfer

1. In Surfer, go to Grid/Grid Node Editor and determine the area in the DEM that needed to be used by writing down the row and column. Close this screen.
2. Next open up Grid/Extract and enter in the file name and click open. The Extract Grid screen will open up and enter in the row and column.
3. The extracted grid file (.grd) can now be converted to XYZ ASCII file through Grid/Convert. Enter the grid name that was extracted and click open. On the Save Grid As screen and "save as type" ASCII XYZ(*dat). This allowed opening the file in the worksheet. This was done for both DEM and Grid files.
4. Go to worksheet and open file, then go to bottom of file and click on cell. This will import the next file to bring in. Next go to File/Import and bring in the other DEM.
5. Then highlight the three columns at the top. Go to Data/Sort and Sort Column C by Ascending.
6. Next delete all the null values in the columns and save the file.
7. Then go to Plot screen and open Grid/Data. Set the spacing to 30.
8. To bring into ER Mapper again Grid/Convert to an ASCII XYZ (.dat) file. Then import in ER Mapper under Utility/Import Gridding Formats/XYZ ASCII.

Table 2.1 Procedure to correct errors with DEM in Surfer.

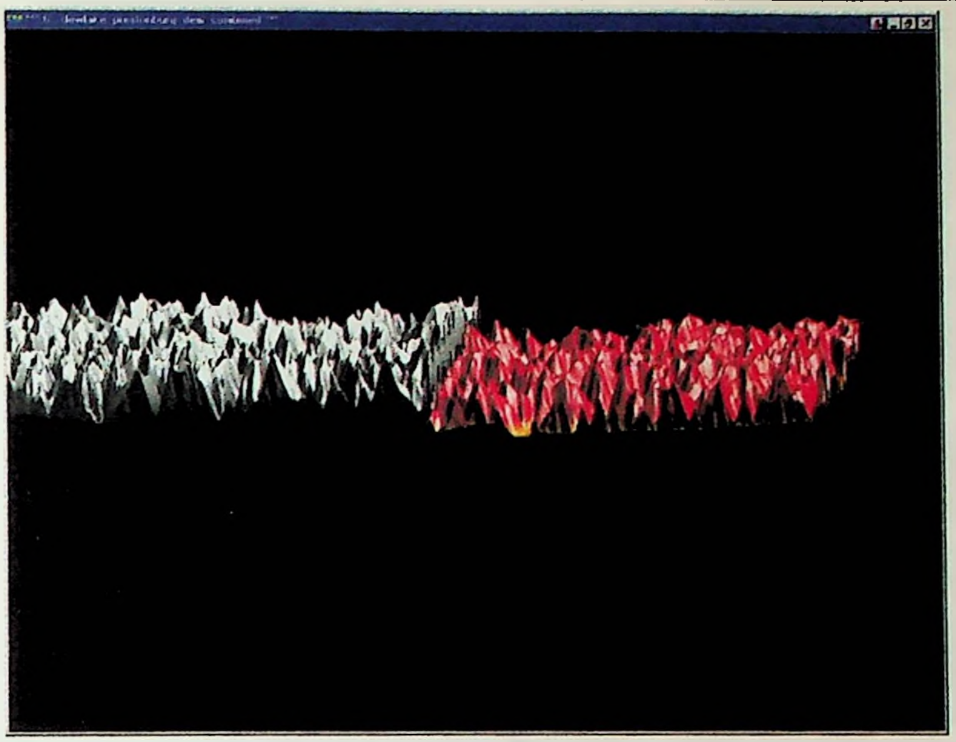

a.

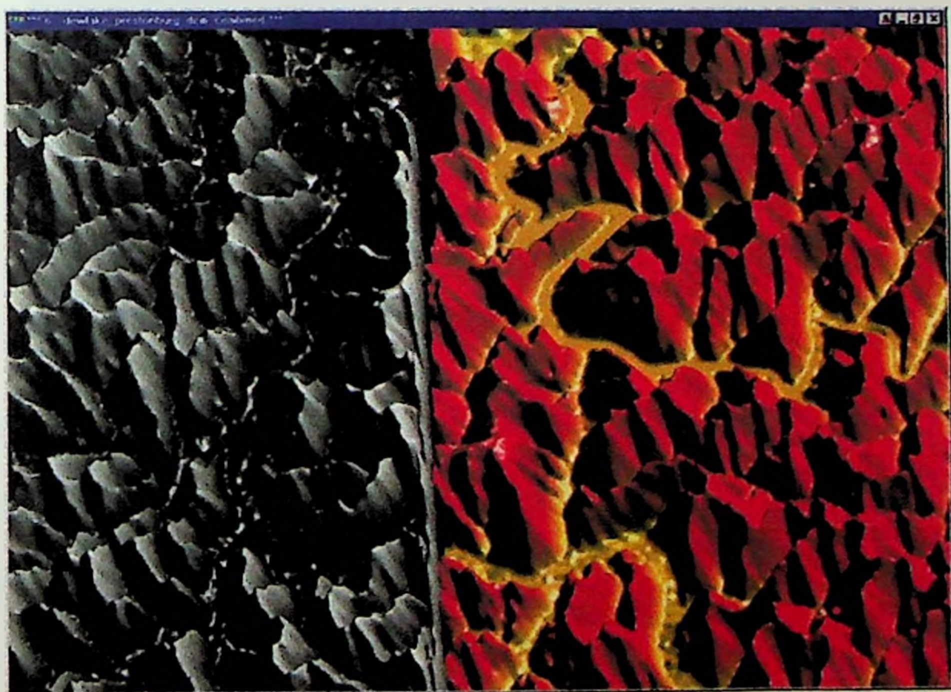

b.

Figure 2.94a and b. Display showing problems with digital elevation models before correction in Surfer. Figure a.is showing problem with elevations. Figure b. demonstrated errors with edges not lining up properly. Display a. and b. in ER Mapper 6.1

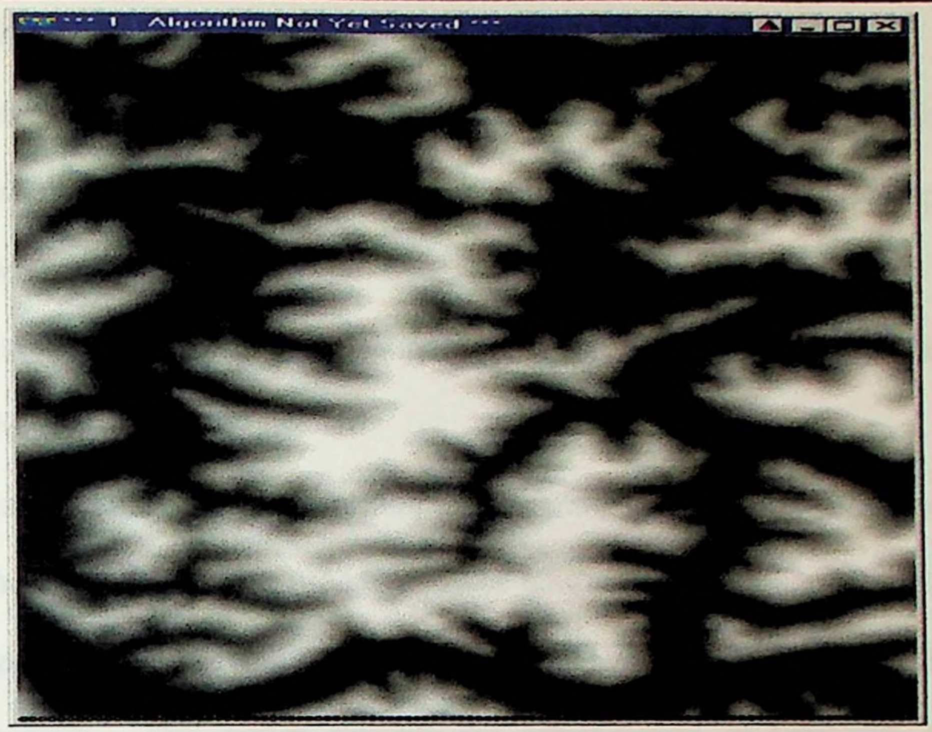

a.

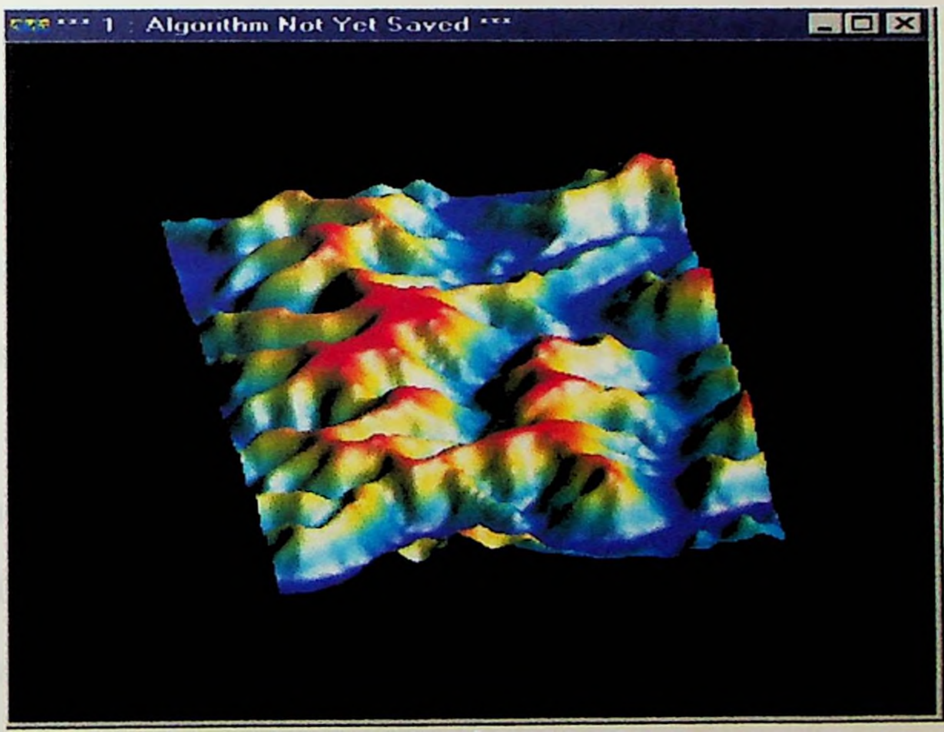

b.

Figure 2.95a and b. Display showing corrected digital elevation models. Figure a.is showing a planametric view. Figure b. Showed the corrected 3-D image. Displays in ER Mapper 6.1

2.11 PRINCIPAL COMPONENT ANALYSIS

Principal Component Analysis (PCA) was used in this study. This statistical form of data compression was used on the information content within six multiple spectra image bands available, reduced to three "principle component" images. This was important in reducing the dimensionality and file size of the multispectral datasets that also improved processing time.

Understanding the representation of new components was important when using (PCA). The term "loads" was used to describe how each band variability was associated with each principle component. This was computed by the correlation of each band with each component. This makes possible the determination of how each band loads variability. Component 1 has the highest loading of variability, component 2 the next highest loading of variability and etc.

To calculate the (PCAs) in ER Mapper the **Formula edit** module was used within the Algorithm dialog. This used raster layers to define and include mathematical functions that combine multi-band data on a point by point basis. A number of common formulae have been supplied with ER Mapper to accomplish processing such as vegetation indexing, supervised classification, ratios and principal components. From the Principle Component menu, select Landsat TM PC1 (Fig 2.96). This loads the principle component following formula into the Generic formula window:

SIGMA (I1..I6))? * PC_COV(I1..I6), R1,)?,1))

This formula generated principal component 1 (PC 1) from all six bands. Principal component 2 (PC 2) was generated by changing the 1 to a 2 in the Generic formula window, so the formula was as follows:

SIGMA (I1..I6))? * PC_COV(I1..I6), R1,)?,2))

Change to 2

Then by selecting the **Apply changes** process to verify the formula syntax. This step was repeated to generate principal component 3 (PC 3). A color composite was created using the (PCAs). The display was PC 1 in blue, PC 2 in green, and PC 3 in red (Figure 2.97). The image was then classified using ISOCLASS unsupervised classification with ER Mapper.

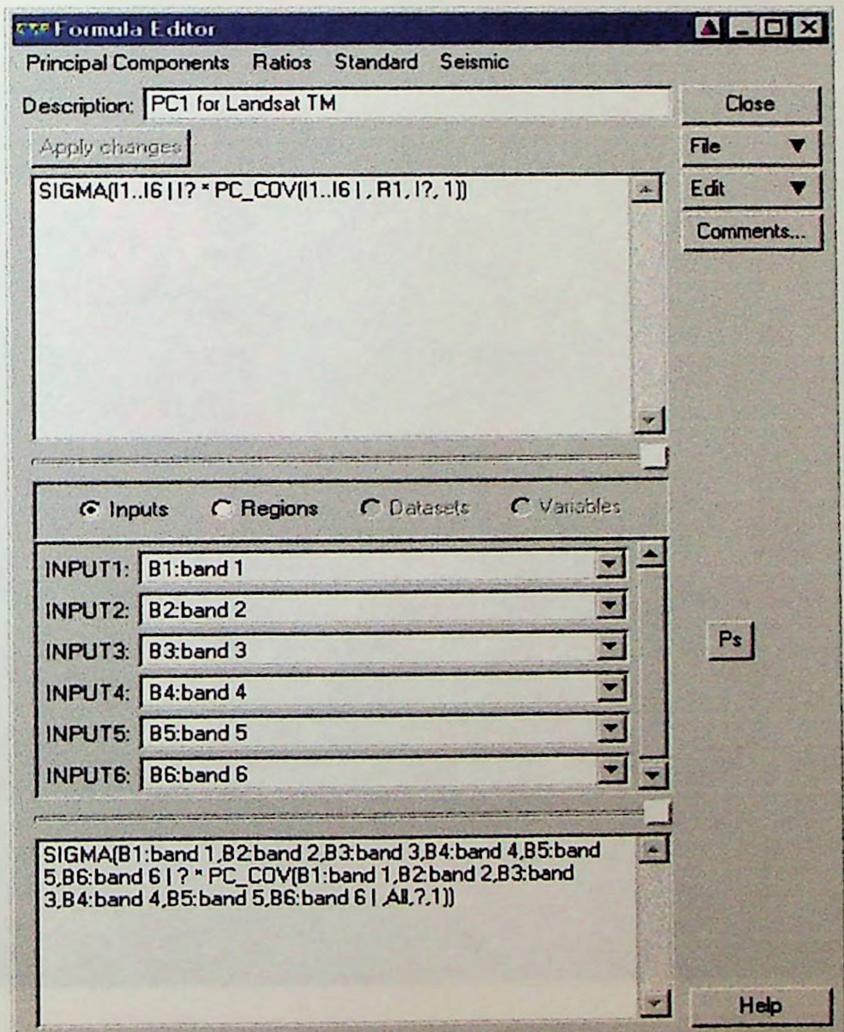

Figure 2.96. Formula Editor in ER Mapper 6.1 showing PCA.

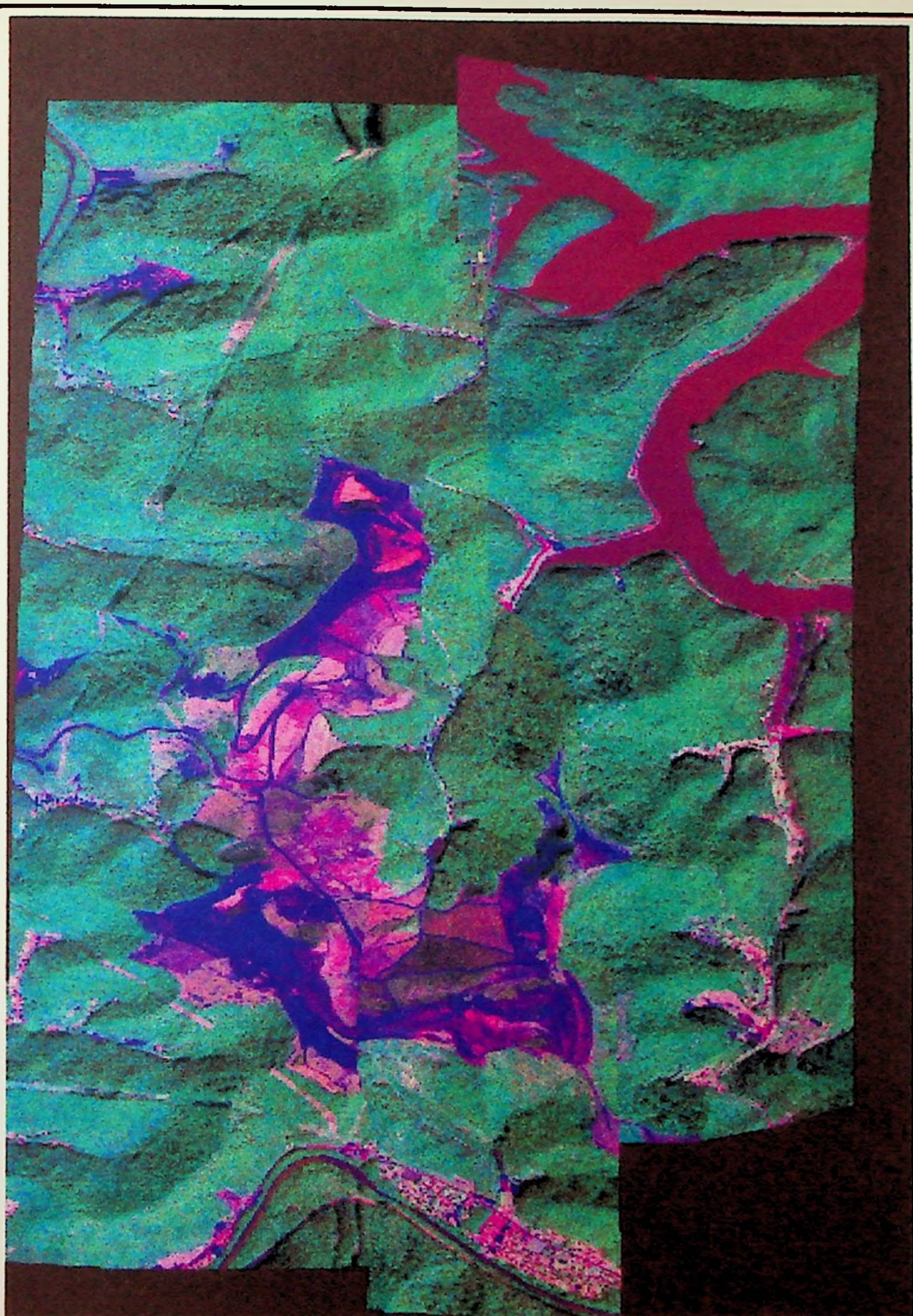

Figure 2.97. Image generated from PC 1 in blue, PC 2 in green, and PC 3 in red using ER Mapper 6.1.

2.12 CLASSIFICATION PROCEDURE

A classification procedure was developed for the mosaicked image. The objective of the analysis was feature extraction in pattern recognition in order to discriminate environmental factors within and around the water body from the surrounding land area or watershed. Water had a very distinct spectral signature that enabled its easy discrimination. In this study six bands were available to identify the extents of the suspended sediment within the water body. Traditionally, researchers and others collect field measurements of water variables at the same time as the satellite or aerial imagery was acquired. In this study there was no ground truth taken at the time the imagery was taken. Therefore, alternative techniques were developed for Dewey Lake. Supervised classification was experimented within combination with unsupervised classification techniques. The general steps required for feature extraction in this project were summarized in Table 2.2. The actual classification was performed using a variety of algorithms for supervised and unsupervised classification.

In the supervised classification, the identity and location of some of the land cover types, such as urban, forest, and mined area, was known previously, through fieldwork experience. Training sites were chosen from homogeneous representative, specific sites for known land-cover types. These areas have spectral characteristics that are known. Area spectra are to be used in the classification algorithm for land-cover mapping for the image.

General Steps Used for Feature Extraction from Digital Aerial Imagery.

Nature of the Classification Problem

- Define environmental parameter
- Identify the classes of interest

Image Processing for Extracting Feature

- Radiometric correction
- Geometric rectification
- Image classification logic
  - Supervised
    -Maximum likelihood
  - Unsupervised
    -ISOCLASS
- Extract data from training sites using most bands
- Select the most appropriate bands using feature selection
  - Statistical
- Extract thematic information
  - By class (supervised)
  - Label pixels (unsupervised)

Error Evaluation

- posteriori knowledge of the study area

Results

- Digital classified 3-D visualization thematic maps

Table 2.2. General Steps required for feature extraction from digital aerial imagery.

2.121 SUPERVISED CLASSIFICATION

The following procedure was for performing supervised classification. By using the annotation tool located under the **Edit menu** in ER Mapper, then selecting **Edit/Create Regions,** the **New Map Composition** dialog box opens. The 'Raster Region' option had to be selected, and Ok selected. In ER Mapper, the **Tools palette** option containing the vector annotation tool was opened. On this module the **Polygon mode** was selected to draw a circle around a representative sample within the coal mining area. The **Map Composition Attribute** module was entered in the name. This procedure was repeated for all training site classes. Selecting the Save file option on the **Tools** module saved the results. Figure 2.98 was an unsupervised classified image that had training regions defined on it was processed as a supervised classification. This was a common hybrid technique to combine unsupervised with supervised classification.

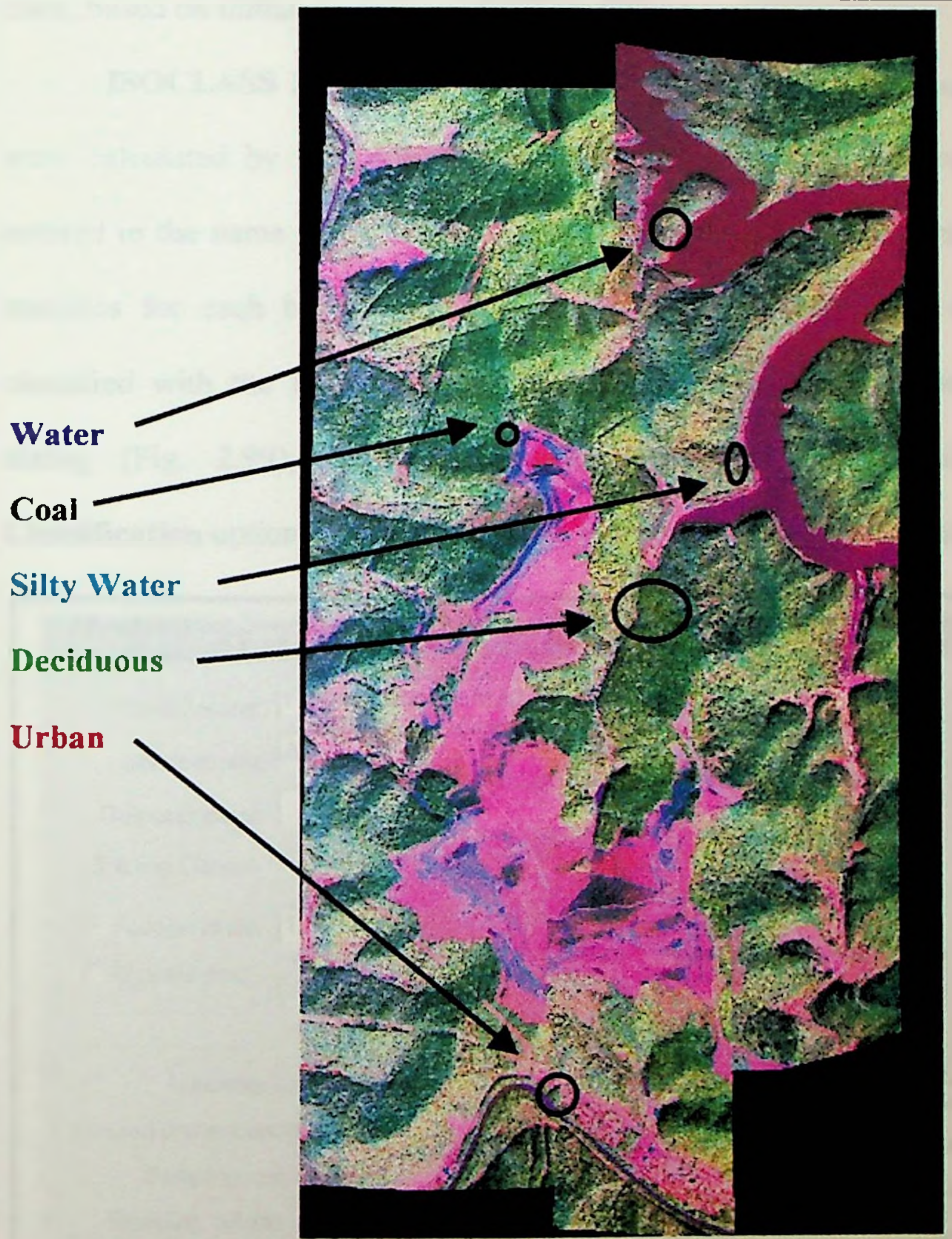

Figure 2.98. An unclassified image displaying training regions located in ER Mapper 6.1.

2.122 UNSUPERVISED CLASSIFICATION

This was an unsupervised method to transform multispectral image data into thematic information classes. The classification program **ISOCLASS** searched for natural groupings or clusters of the spectral properties of each pixel, and assigned it to a class, based on initial clustering parameters defined.

ISOCLASS first calculated statistics for the image to be classified. Statistics were calculated by first selecting **Calculate Statistics** from the **Process** menu, and entered in the name of the file to be calculated. The computer program calculated the statistics for each band. Once the statistics were calculated, the dateset could be classified with the **ISOCLASS** method. To open the **Unsupervised Classification** dialog (Fig. 2.99), from the **Process menu**, the **Classification/Unsupervised Classification** option was selected. Next, the input dataset name and output dataset name

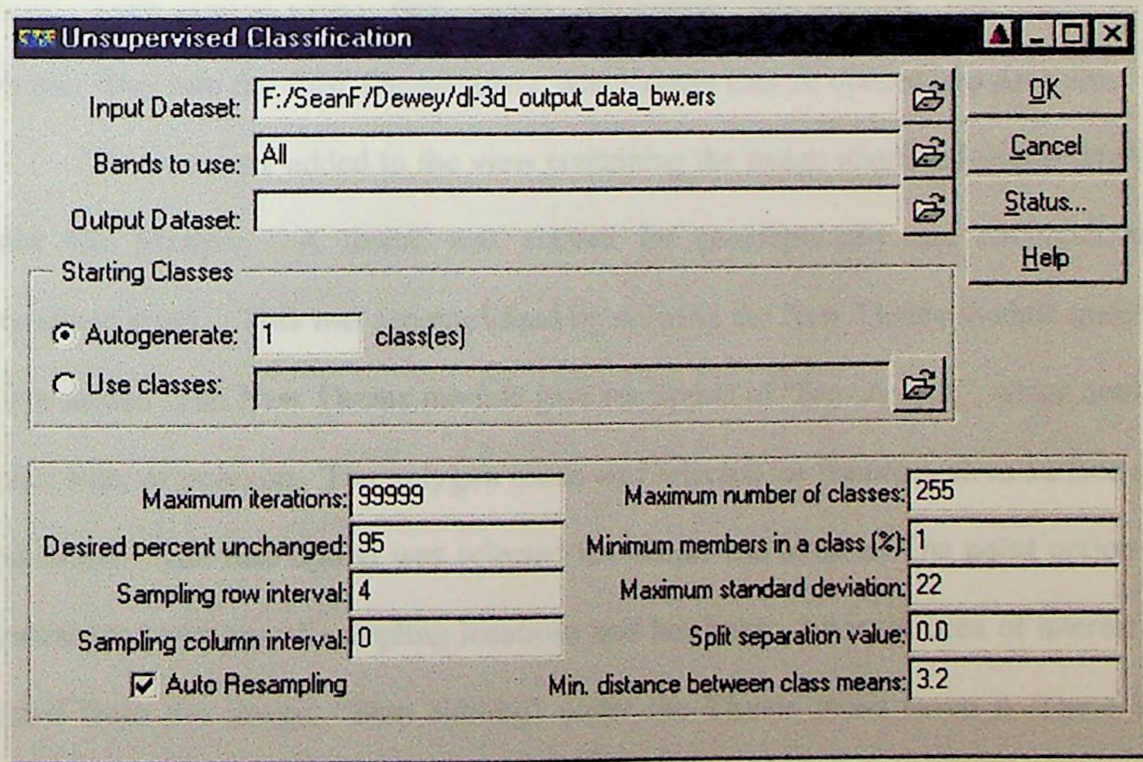

Figure 2.99. Unsupervised classification window in ER Mapper 6.1. This showed the parameter setup used in this study.

were entered. The method employed to set up the parameters for **ISOCLASS** utilized the **maximum standard deviation,** divided it by two and set the **Minimum number in a class** to 1.0, while setting the **Desired percent unchanged** to 95.0 and **Sampling row interval** to 4. This helped to lower the number of classes to a manageable number and decreased processing time.

2.13 ER MAPPER INPUTS TO ARCVIEW

The digital aerial remotely sensed data in ER Mapper was interfaced with ArcView via a 'plugin' available for ArcView. The 'plugin' was download from ER Mappers home page (www.ermapper.com). Once the 'plugin' was installed images created within ER Mapper could be accessed and displayed in ArcView. In ArcView under File menu the **Extensions** module was selected followed by selecting ECW v2.0 and ER Mapper Images. A new view was selected and the **Add Theme** module opened. In the "Data Source Types" box "Image Data Source" was selected. This loaded all ER Mapper files into the **Add Theme** menu, which could then be opened into ArcView.

Themes were added to the view containing the image interfaced within ArcView from ER Mapper. A theme was created for geographically and environmentally important areas. This was accomplished by utilizing the **New Theme** module under the View menu. The **New Theme** module gave the option of "Feature type", which could be point, line, or polygon. The **polygon** mode was selected for feature such as surface mine and forest. The **line** option was selected for streets and streams. The **point** option was chosen for locations of sampling locations and hot links. After the area of interest was traced from the image, "Stop Editing" under the **Theme** menu saved it. These steps created figure 2.991 in ArcView 3.1. The hot link feature in ArcView 3.1 was then used

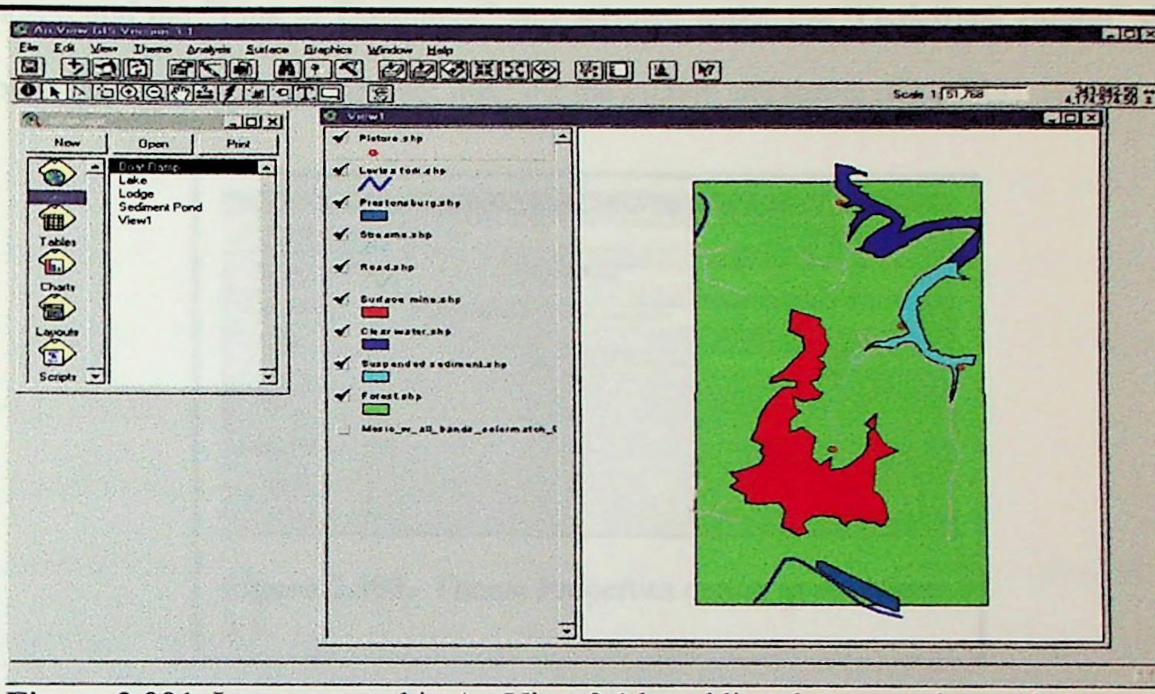

Figure 2.991 Image created in ArcView 3.1 by adding themes such as polygon, line and point.

to link sample location with field photograph of vegetation. The photos taken from sample location were first brought into ArcView 3.1 by adding a theme to a new view, which contained the photo. Then with the theme created with the sample locations opened the **Open Theme Table** module was selected. Next from the Table menu, "Start Editing" was selected. The **Add Field** module was selected for the **Edit** menu (fig. 2.992). In this dialog box was typed the name of the new field "Photo" and from the dropdown list, "String" was selected. Next the **Edit Tool** module was selected and the name of the views created earlier were typed in the photo field for the corresponding sample location. The **Theme Properties** module was opened and the **Hot**

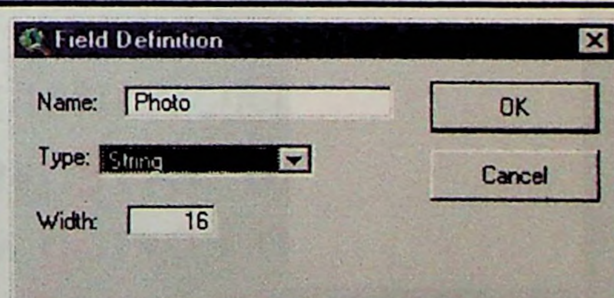

Figure 2.992. Field Definition module in ArcView 3.1.

Link module was selected (fig 2.993). From the Field drop-down list "Photo" was chosen and the "Link to Document" was selected under the "Predefined Action" drop-down list. This completed the hot links for the Picture site theme (fig 2.994).

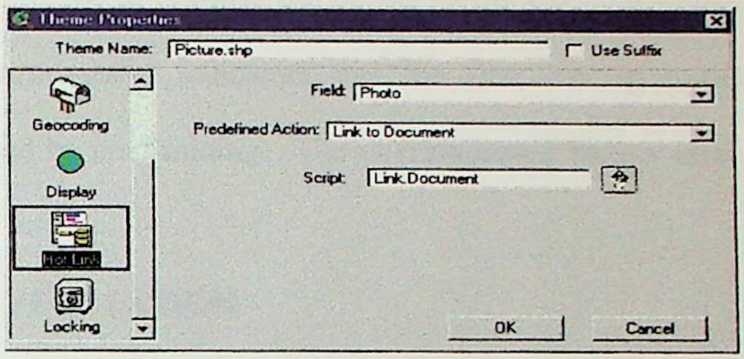

Figure 2.993. Theme Properties dialog in ArcView 3.1.

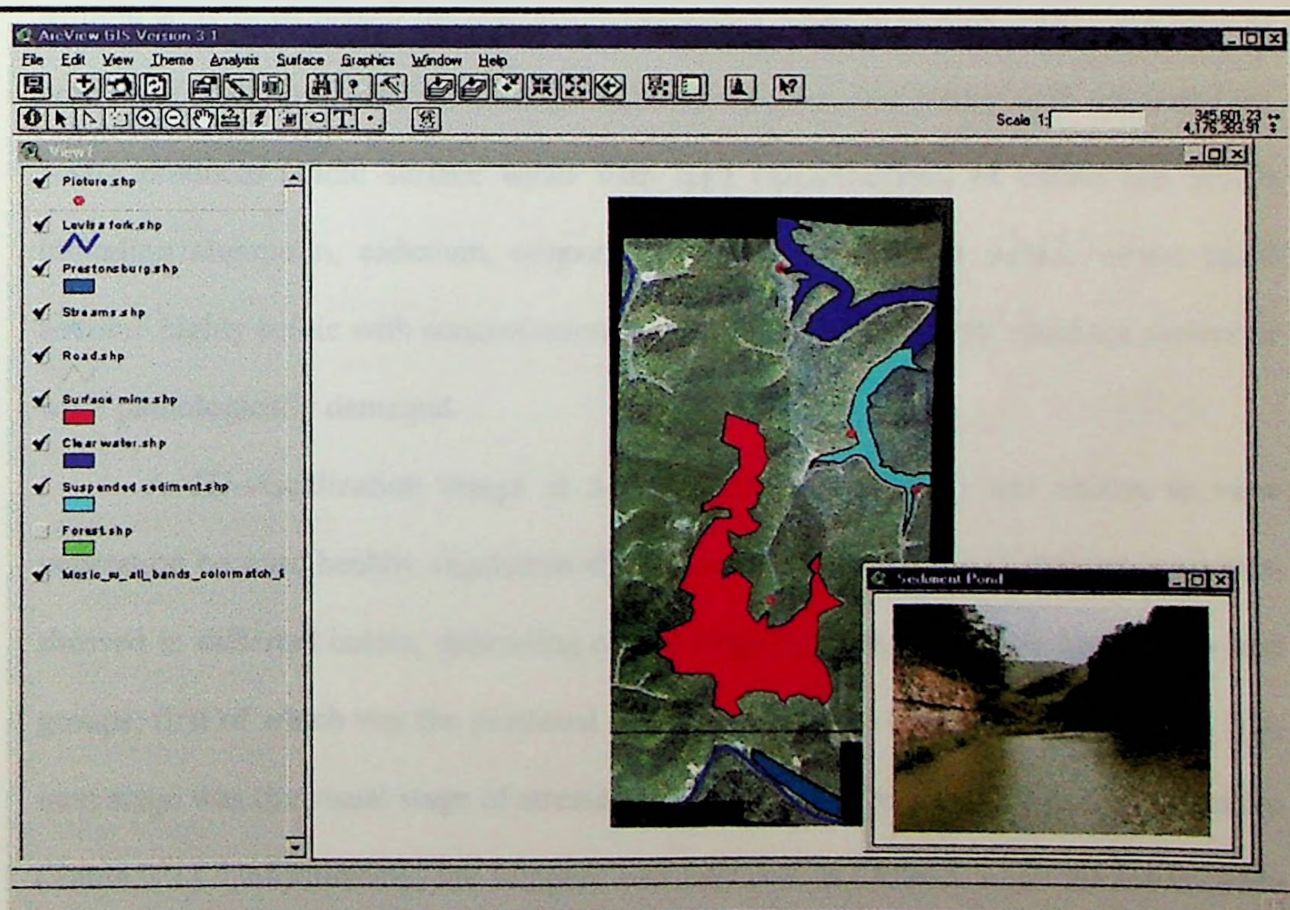

Figure 2.994. A view with a photo of the sediment pond hot linked in ArcView 3.1.

Chapter Three

RESULTS AND DISCUSSION

Of the different parameters influencing lake morphology, several combinations of techniques were utilized to evaluate the impact of mining activity on Dewey Lake. The selection of environmental indicators was the first task in studying environmental degradation caused by coal mining. The environmental factors used for the study area are discussed.

3.1 STRESSED VEGETATION

Remotely sensed data provided a powerful tool for inspecting stressed vegetation on a large scale. Specific interest was damage to vegetation from surface mining activity. Mining activity increased the interaction of surface water with high sulfur coal forming acid mine drainage (AMD) when high sulfur coal comes into contact with water and air. AMD produces acidic surface water with high concentrations of sulfate and metals including aluminum, cadmium, copper, iron, and zinc. These surface waters could become highly acidic with concentration of minerals such that plants could not survive or were pathologically damaged.

A 3D-visualization image in a color infrared (Fig 3.1) was chosen to view vegetation because healthy vegetation showed well as a red color and stressed vegetation showed in different colors, depending on the stage of stress. This was broken into two groups, first of which was the previsual stage this displayed in a pink to blue color. The next stage was the visual stage of stressed vegetation. This was displayed in a cyan color (Table 3.1). Unfortunately, the imagery was captured in October when the leaves were going through senescence, changing colors, which complicated the issue of classification

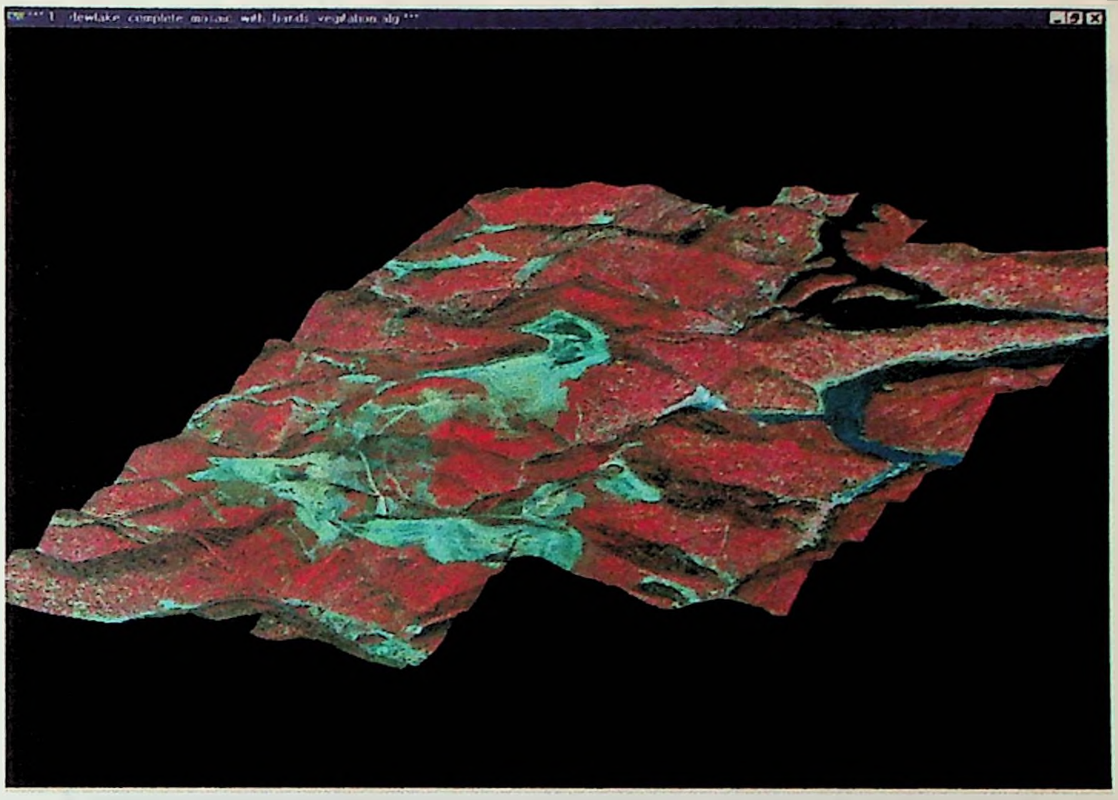

Figure 3.1 3-D visualization model displayed in color infrared (CIR), created in ER Mapper 6.1.

because the stressed vegetation and senescence have similar spectral signature. Figure (3.2) below was an enlarged view of a color composite and a false color IR image around

Subject	Normal	Color Infrared (CIR)
Healthy Vegetation:		
Broadleaf Type	Green	Red to magenta
Needle-leaf type	Green	Reddish Brown to purple
Stressed Vegetation:		
Previsual stage	Green	Pink to blue
Visual stage	Yellowish green	Cyan
Autumn leaves	Red to yellow	Yellow to white
Clear water	Blue to Green	Dark blue to black
Silty water	Light green	Light Blue
Red bed out crops	Red	Yellow

Table 3.1 Terrain signature on normal color images and color infrared images. (Modified from Sabins 1997).

a settling pond that were of the same scale to demonstrate the effect of vegetation senescence in the color IR image. This effect made the detection of stressed vegetation

a.

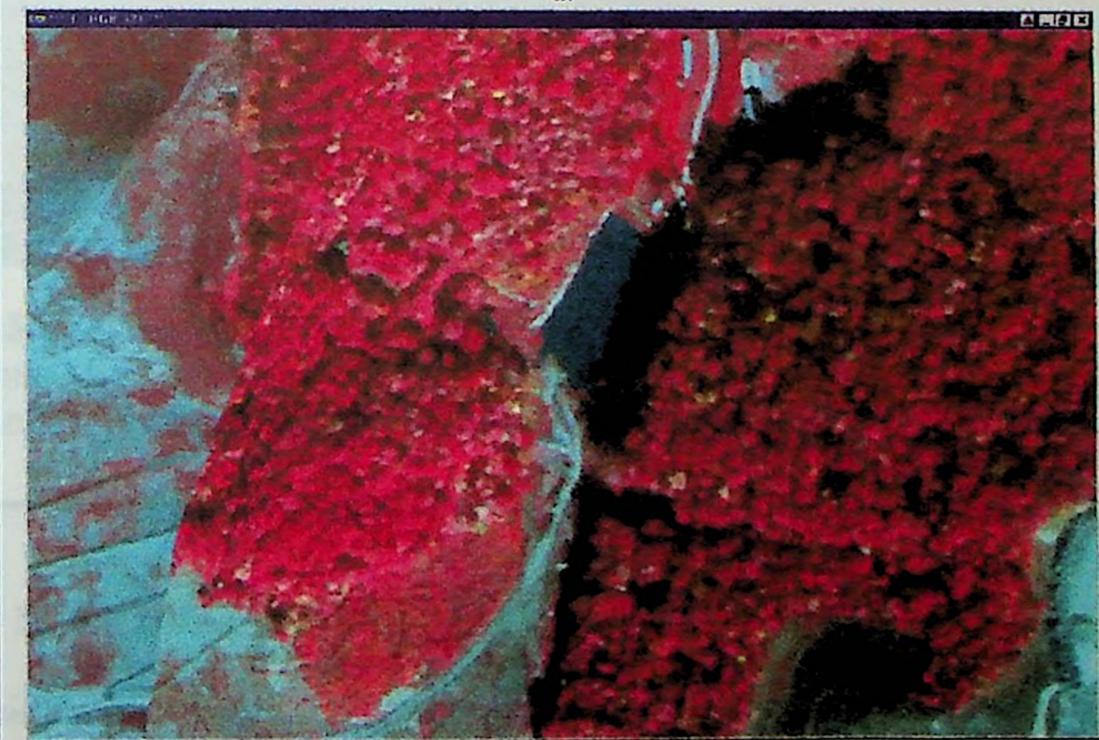

b.

Figure 3.2. The first image a. is a color composite showing fall foliage. The second image b. is a CIR of the same area demonstrating the effect of senescence. Displayed in ER Mapper 6.1

difficult to identify and classify. Figure (3.3) shows the mining operation at Stratton

Branch. Stressed vegetation was not identified as a result of acid mine drainage because of confusion with fall leaf senescence. This would have shown up in a pink to blue color around the mining area.

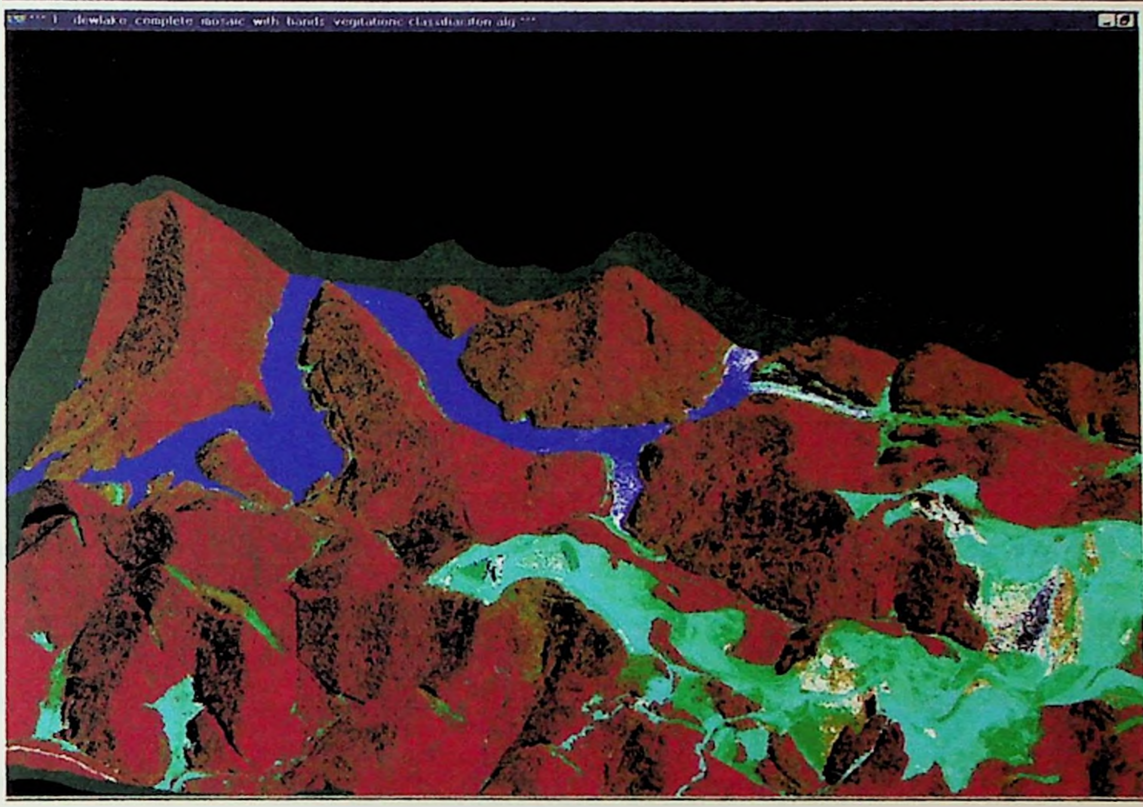

Figure 3.3. Classified 3-D visualization composite image illustrating mining operation. Mine operation in shades of green. Stressed vegetation in association with mining confused with fall leaf senescence. Displayed in ER Mapper 6.1.

3.2 ACID MINE DRAINAGE

Acid mine drainage results when the mineral pyrite (FeS_2) was exposed to air and water resulting in the formation of sulfuric acid and iron hydroxide. Pyrite was commonly present in coal seams and associated rock layers. Acid mine drainage formation occurs during surface mining when overlying rocks are broken and removed to obtain the coal. Surface mining could devastate water resources by lowering the pH and coating stream bottoms with iron and aluminum hydroxides.

Several techniques were examined to evaluate the extent of contamination from Acid mine drainage. The first was to construct a color 3-D geobiophysical image model for selected locations enlarged to visually examine for iron staining (yellow boy). The enlarged views provided no evidence of "yellow boy" for the chosen locations shown in Figure (3.4).

The next method for locating acid mine drainage was to photo interpret the image for stressed vegetation around streams entering the lake. Stressed vegetation would be a possible indicator of acid mine drainage. The same sample locations as Figure 3.4 were chosen in the examination for stressed vegetation in a color infrared image (Fig 3.5). The results were negative indicating that vegetation was not influenced discernibly by a lower pH due to acid mine drainage. This was because the fall colors could be masking any noticeable effects.

3.3 SUSPENDED SEDIMENT LOAD

Acid mine drainage often contained high levels of dissolved metals and sediment. Sedimentation quilts the bottom of the steam channel making breeding and feeding for species of fish and benthics difficult or impossible. Elevated levels of metals such as aluminum were toxic to aquatic life. These conditions could degrade many portions of the Dewey Lake to the point where no aquatic life could exist. Table (3.1) was especially useful in helping to delineate some import environmental factors on the imagery. For example in Figure 3.1 there was a pronounced colorshift in Dewey Lake. The water was light blue where Stratton Branch was entering the lake. Farther away the coloration was

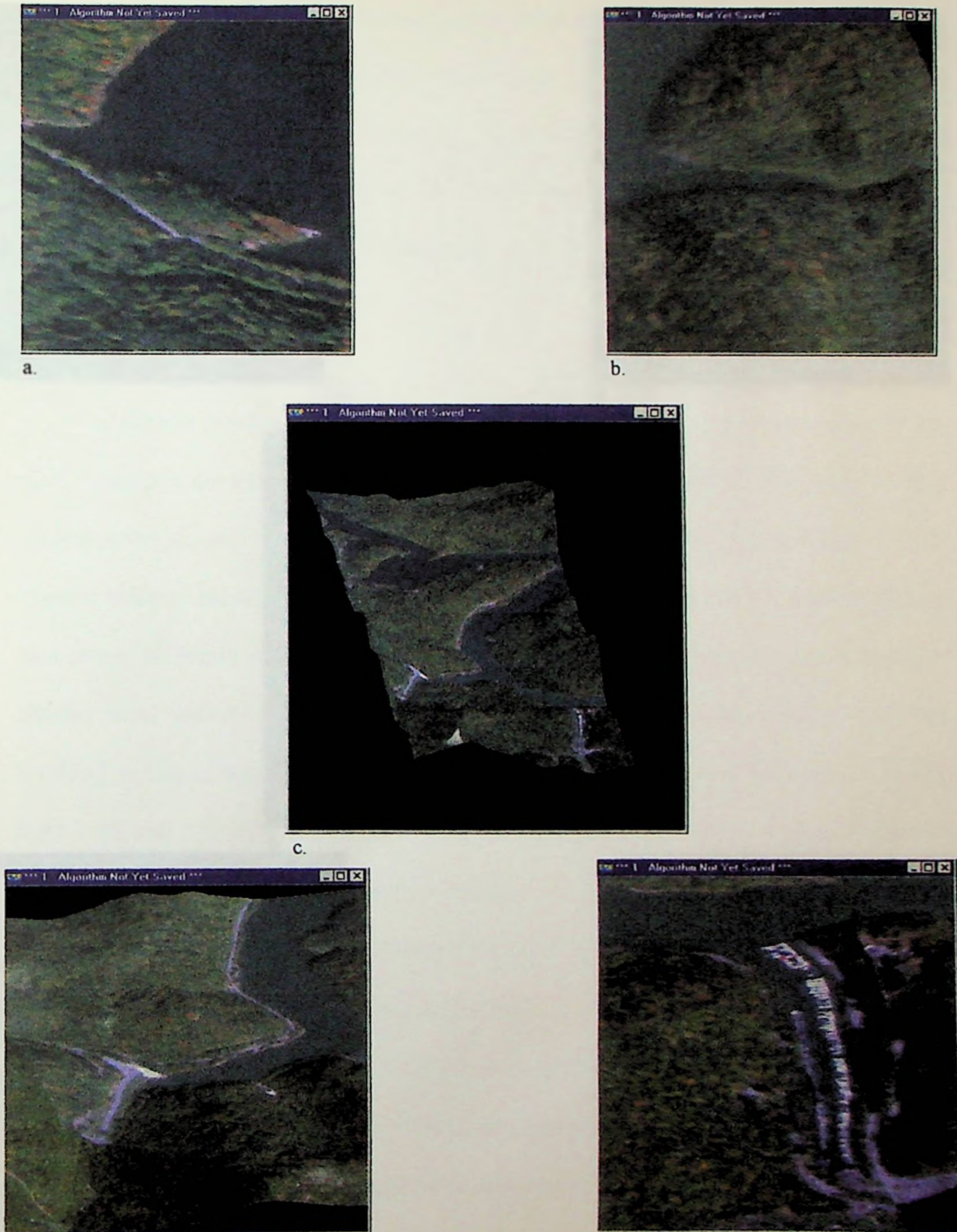

Figure 3.4. Color composite 3-D geobiophysical model (c.) with enlarged areas (a, b, d, and e) to visually examine for acid mine drainage in ER Mapper 6.1.

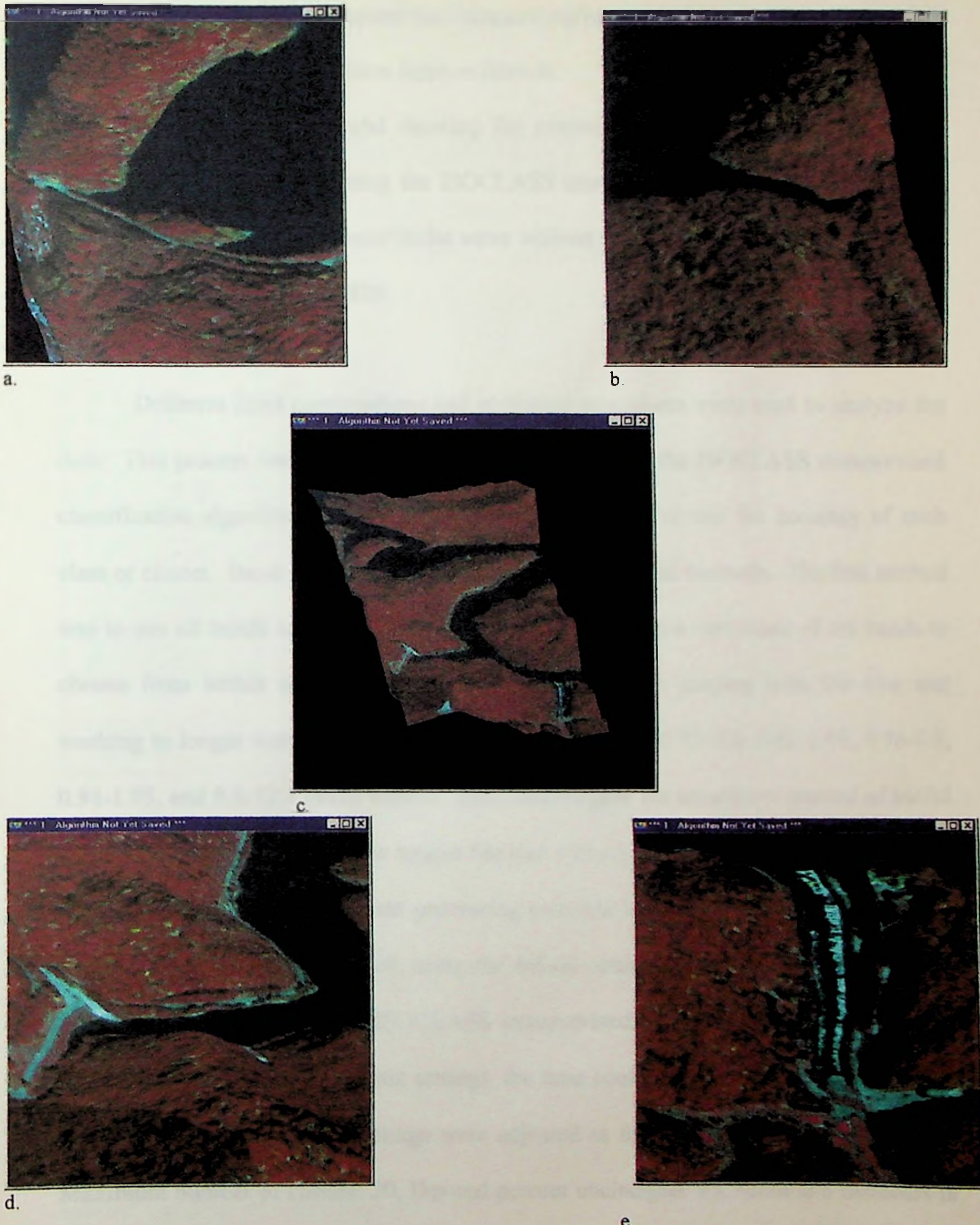

Figure 3.5. CIR 3-D geobiophysical model (c.) with enlarged areas (a, b, d, and e) to visually examine for stressed vegetation associated with acid mine drainage. Created in ER Mapper 6.1.

darker blue to black. This showed the increased sediment load coming from the surface mine which entered the lake from Stratton Branch.

A geobiophysical model showing the extents of the suspended sediment was created. This required adjusting the ISOCLASS unsupervised classification module to highlight the suspended sediment in the water without creating too many clusters.

3.4 FEATURE EXTRACTION

3.41 ALL BANDS

Different band combinations and statistical procedures were used to analyze the data. This process was then tested in ER Mapper utilizing the ISOCLASS unsupervised classification algorithm. The results were then displayed to test the accuracy of each class or cluster. Band combinations were chosen from several methods. The first method was to use all bands supplied with the imagery. There was a maximum of six bands to choose from within each dataset. The band wavelengths starting with the blue and working to longer wavelengths were as follows 0.45-0.52, 0.52-0.6, 0.63-0.69, 0.76-0.9, 0.91-1.05, and 8.5-12.5 micro meters. This method gave the maximum amount of useful information, but also created the largest file size with an average 128.6 megabytes before processing. This amount of data processing required 12 hours on twin Intel 400 MHz processors, and windows NT 4.0, using the default settings, or more time, depending on the parameters chosen in the ISOCLASS unsupervised classification module, but with proper adjustments to the statistic settings, the time could be decreased to approximately one half-hour. The default settings were adjusted as follows: Maximum iterations: 20, Maximum number of classes: 30, Desired percent unchanged: 95, Minimum members in a class (%): 1, Sampling row interval: 4, Maximum standard deviation: 10, Sampling column interval: 4, and the auto resampling was selected. Other settings were left to the default settings (Fig 3.6).

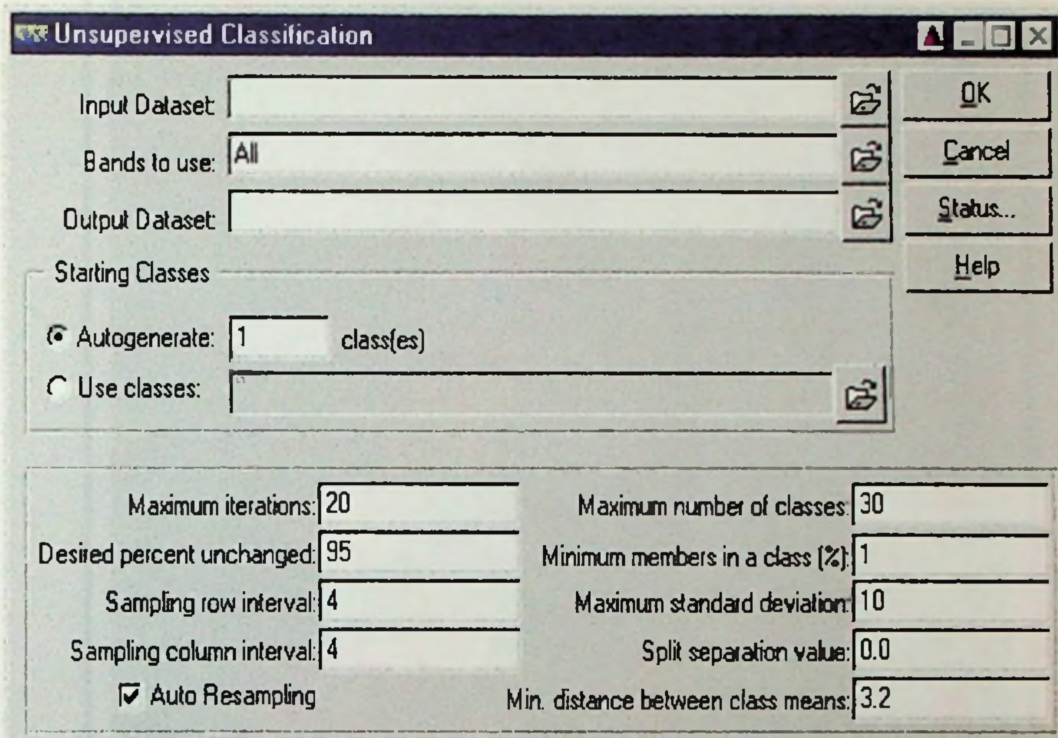

Figure 3.6. Unsupervised classification module, displayed with proper adjustments to parameter settings in ER Mapper 6.1.

Figure 3.7 was a classified mosaic with all bands included in the classification. The image was first colormatched using ER Mappers balancing wizard. The limits were clipped to 99%. The dataset created was used in the ISOCLASS unsupervised classification. Note the good separation in Figure 3.5 between the clear water in Dewey lake and the water with a heavy suspended sediment load closer to the surface mine. This resulted from the spectral similarities between urban areas and barren soil relating to the surface mining operation. Another area of confusion in classification was with the spectral signature of water and coal.

Figure 3.7. Classified mosaic created in ER Mapper 6.1 with all bands included in processing.

3.42 ALL BANDS WITH DEM

ER Mapper had the ability to incorporate DEM data into the ISOCLASS unsupervised classification. Topography was valuable in classification within mountainous terrain. The spectral signature observed within Figure 3.7 previously between the urban and surface mine were very similar.

Another image created used the same raw dataset as in Figure 3.7. It had the same parameters setup but included the DEM as a band of information to be processed with the ISOCLASS unsupervised classification. This created the classified image in Figure 3.8, that increased the separability displayed in the coal and water. This process

Figure 3.8. Classified image created in ER Mapper 6.1 with all bands including a height band.

also increased the separability between urban and surface mines as shown in Figure 3.9. Including the DEM data as a band of information created the most accurate model (Fig 3.10 and 3.11).

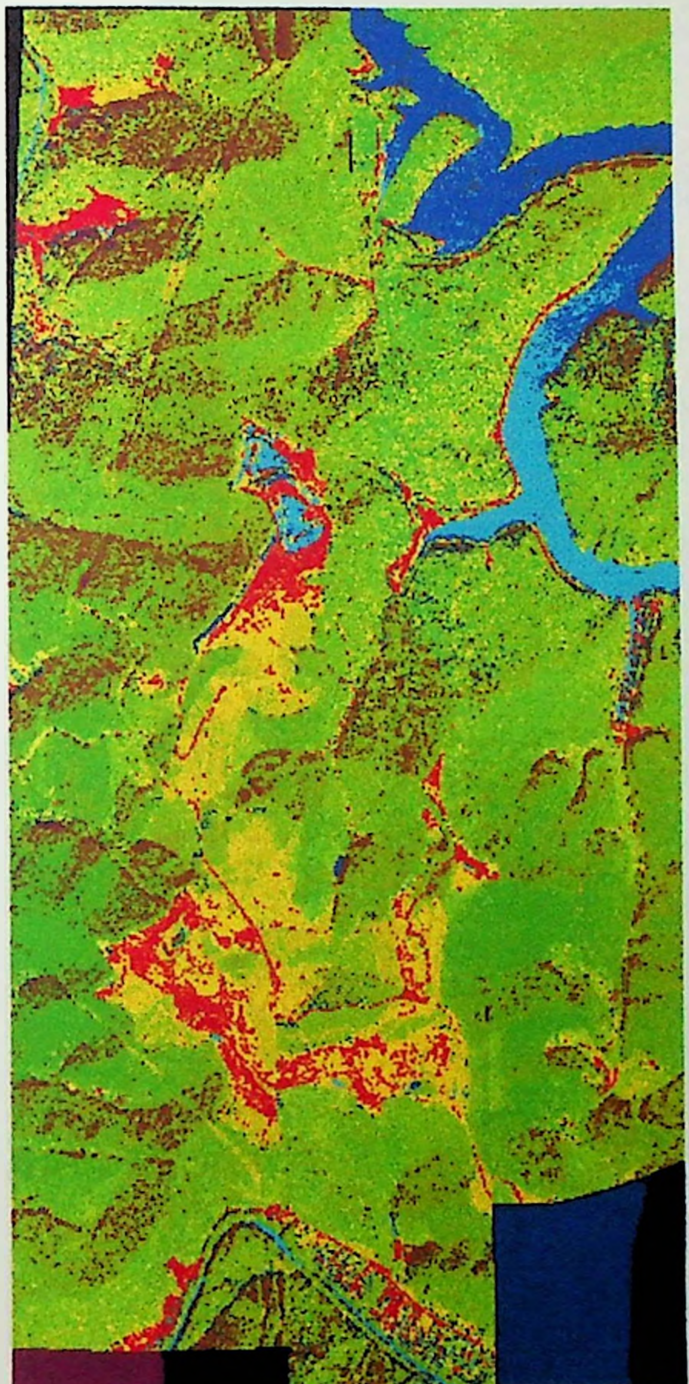

a.

b.

Figure 3.9. Side by side comparison of classified mosaic images. Figure a. was processes with all band. Figure b. was processed with all bands including a height dataset.

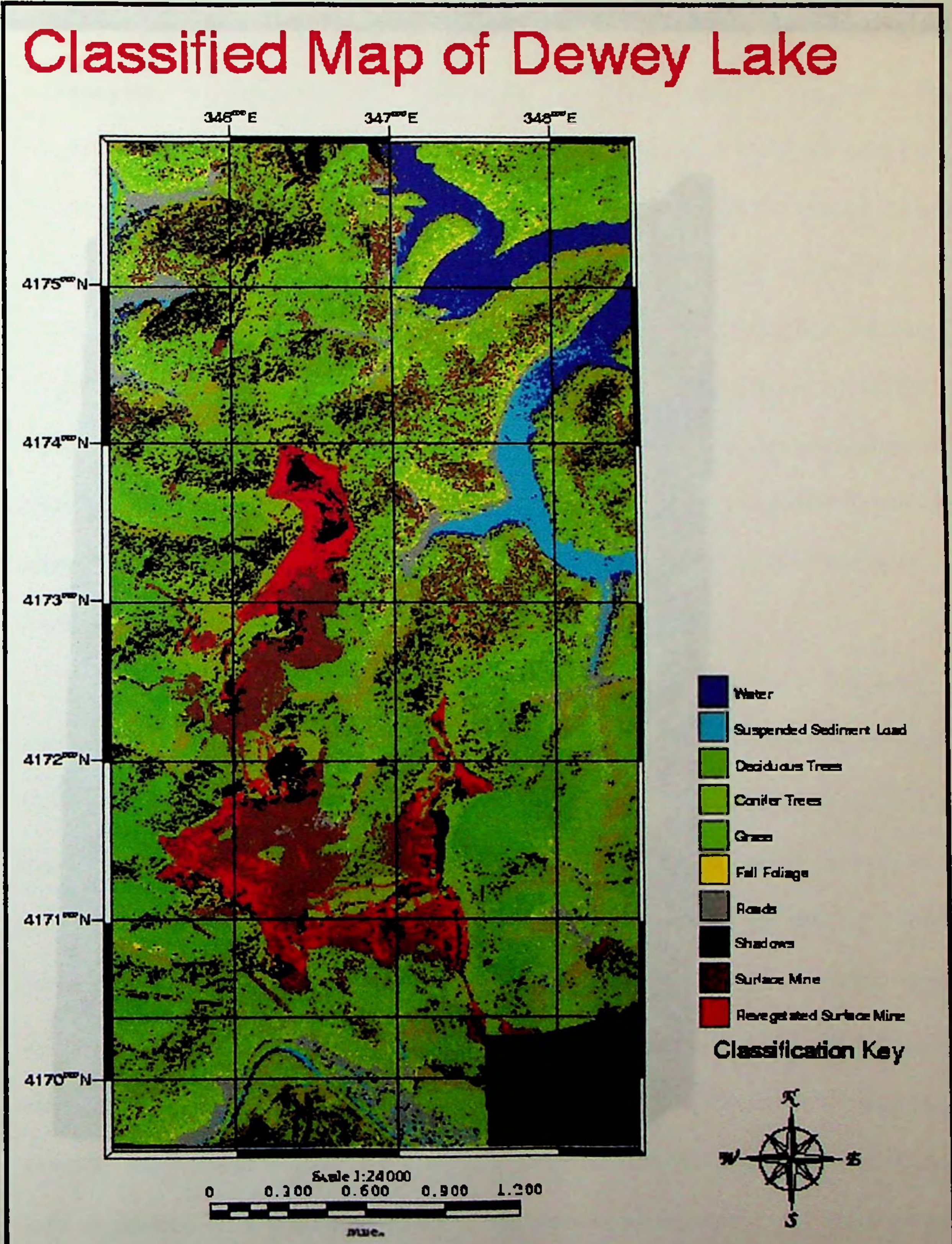

Figure 3.10. Completed classified map created with all bands plus a height layer. Created in ER Mapper 6.1.

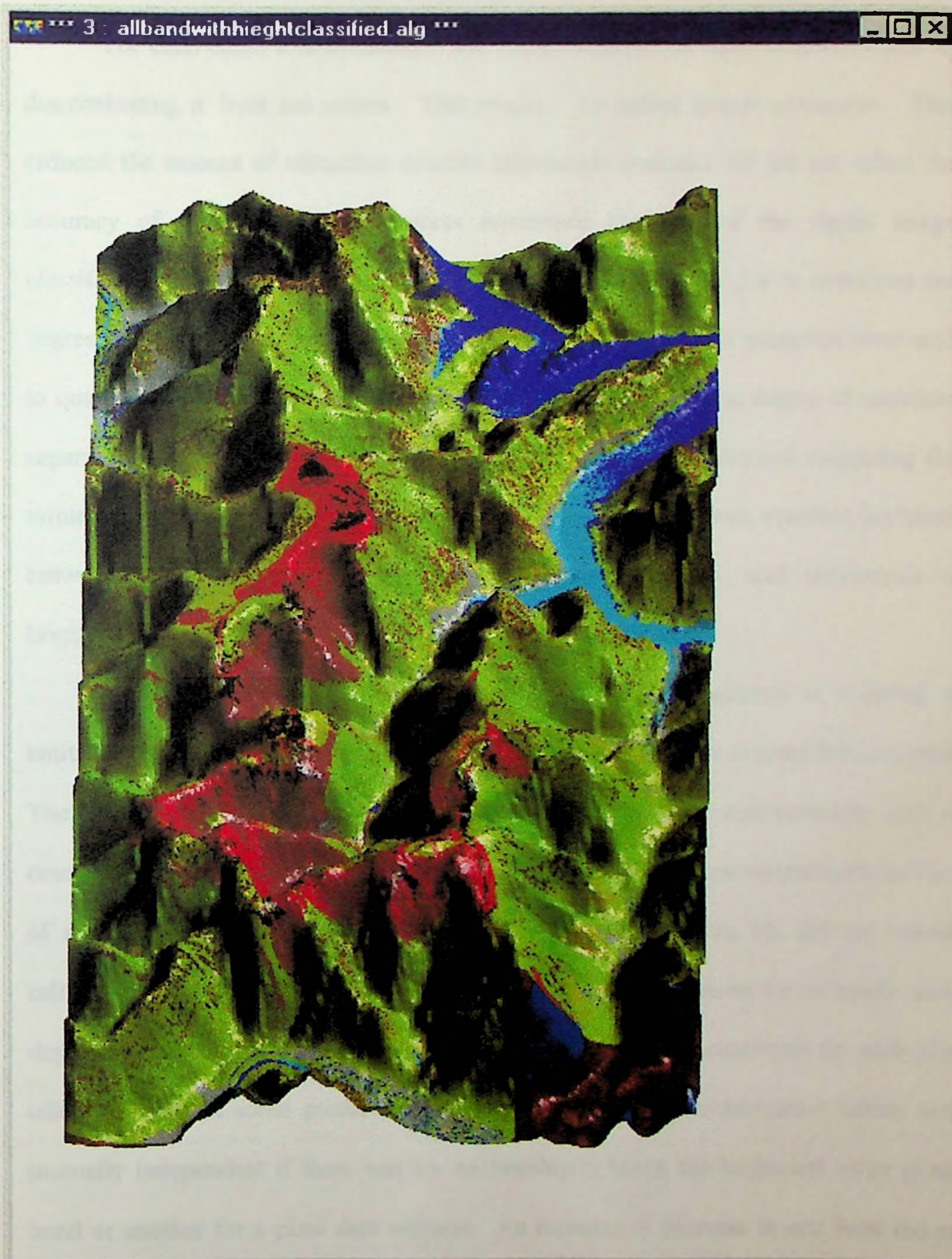

Figure 3.11. Same image as figure 3.8 displayed in 3-D.

3.43 OPTIMUM BANDS SELECTION

For each class, a determination was made to select the most effective bands in discriminating it from the others. This process was called feature extraction. This reduced the amount of redundant spectral information analyzed but did not affect the accuracy of the results. This process minimized the time of the digital image classification process. Feature extraction involved statistical analysis to determine the degree of between-class separability. Statistical methods of feature extraction were used to quantitatively select which subset of bands provides the greatest degree of statistical separability between any two classes (see Table 3.2). This involved computing the minimum and maximum values for each band of imagery, the mean, standard deviation, between band variance-covariance matrix, correlation matrix, and frequencies of brightness values (Jahne, 1991; Jensen et al., 1993).

This study used remotely sensed multispectral measurements of reflected or emitted light from environmental objects influencing Dewey Lake in more than one band. Therefore it was useful to look at the multivariate statistical measurements such as covariance and correlation matricies among the six bands. The univariate statistics were of minimum, maximum, mean, median and standard deviation, but did not provide information concerning whether or not the spectral measurements in the six bands varied dependently or independently. In remote sensing spectral measurements for each pixel often changed in some predictable manner. The spectral measurement values were mutually independent if there was no relationship between the brightness value in one band or another for a pixel data element. An increase or decrease in one band did not produce an increase or decrease in another band. Because of this independence, a

STATISTICS FOR DATASET: dewlake_complete_mosaic_with_dataset.ers
REGION: All

	Band1	Band2	Band3	Band4	Band5	Band6
Non-Null Cells	10347264	10347264	10347264	10347264	10347264	10347264
Area In Hectares	1055.416	1055.416	1055.416	1055.416	1055.416	1055.416
Area In Acres	2607.990	2607.990	2607.990	2607.990	2607.990	2607.990
Minimum	0.000	0.000	0.000	0.000	0.000	0.000
Maximum	255.000	255.000	255.000	255.000	255.000	255.000
Mean	71.443	76.686	59.914	61.552	65.025	70.316
Median	62.000	70.000	50.000	60.000	66.000	68.000
Std. Dev.	51.529	48.571	42.143	29.465	27.294	36.764
Std. Dev. (n-1)	51.529	48.571	42.143	29.465	27.294	36.764
Corr. Eigenval.	3.932	1.495	0.411	0.097	0.041	0.023
Cov. Eigenval.	7404.246	1471.563	564.883	226.859	62.815	24.811

Correlation Matrix	Band1	Band2	Band3	Band4	Band5	Band6
Band1	1.000	0.906	0.911	0.246	0.257	0.643
Band2	0.906	1.000	0.961	0.439	0.431	0.677
Band3	0.911	0.961	1.000	0.307	0.316	0.649
Band4	0.246	0.439	0.307	1.000	0.962	0.446
Band5	0.257	0.431	0.316	0.962	1.000	0.498
Band6	0.643	0.677	0.649	0.446	0.498	1.000
	Determinant			0.000		

Covariance Matrix	Band1	Band2	Band3	Band4	Band5	Band6
Band1	2655.270	2267.138	1978.717	373.275	360.924	1217.331
Band2	2267.138	2359.154	1966.653	628.957	572.007	1209.329
Band3	1978.717	1966.653	1776.027	381.355	363.895	1004.814
Band4	373.275	628.957	381.355	868.164	773.823	483.200
Band5	360.924	572.007	363.895	773.823	744.989	499.335
Band6	1217.331	1209.329	1004.814	483.200	499.335	1351.573
	Determinant		2176124492533634.700			

Cov. Eigenvectors	PC1	PC2	PC3	PC4	PC5	PC6
Band1	0.567	-0.313	-0.038	0.760	-0.034	-0.024
Band2	0.552	-0.031	-0.246	-0.401	0.652	0.216
Band3	0.471	-0.172	-0.151	-0.466	-0.689	-0.183
Band4	0.154	0.656	-0.273	0.125	0.095	-0.668
Band5	0.146	0.611	-0.163	0.143	-0.296	0.686
Band6	0.327	0.259	0.902	-0.092	0.036	-0.051

Table 3.2. Statistics for Dewey Lake Mosaic from ER Mapper 6.1.

measure of their mutual interaction was used. This measure was covariance which was the joint variation of two variables about their common mean. The correlation coefficient was a ratio, and a unitless number. This was used to estimate the degree of interrelation between variables in a manner not influenced by measurement units. Therefore the correlation coefficient ranged from +1 to –1 where a correlation coefficient of +1 indicated a very high correlation relationship between the brightness values of two bands and conversely, a correlation coefficient of –1 indicated that the two bands had high inverse correlation.

The data shown in table 3.2 illustrated a low correlation and covariance for bands 2, 3, and 5, which have been highlighted and underlined. Band 2 was chosen first because of it ability to highlight low pH and iron oxide.

3.44 PCA SELECTED BANDS

The result of the calculated statistics table (Table 3.2) indicated the bands that were correlated with each principal component. For example, the highest covariance (loading) for principle component 1 were for bands 1, 2, and 3 (0.567, 0.552, and 0.471, respectively, (Table 3.2) suggesting that this component was in the visible bands. Conversely, principle component 2 had high loading in the near infrared bands 4 and 5 (0.656 and 0.611), and component 3 had high loading in the thermal band 6 (0.902). Therefore, to include all bands of information into the principal component image, PCA's 1, 2, and 3 were combined for classification to compare the results against the classified image with all bands. Figure 3.12 was a comparison between two images, one created with all three PCAs, and the other with PCA 1 and 2 leaving out the third. The image created with a combination of PCA 1 and 2 shows improvement in classification over the PCA combination of 1, 2, and 3. Note that in Figure 3.12 a. there was no separation between the clear and sediment water because most of the information about the water was located in PCA 1. PCA 1 contained most of the information from the visible region.

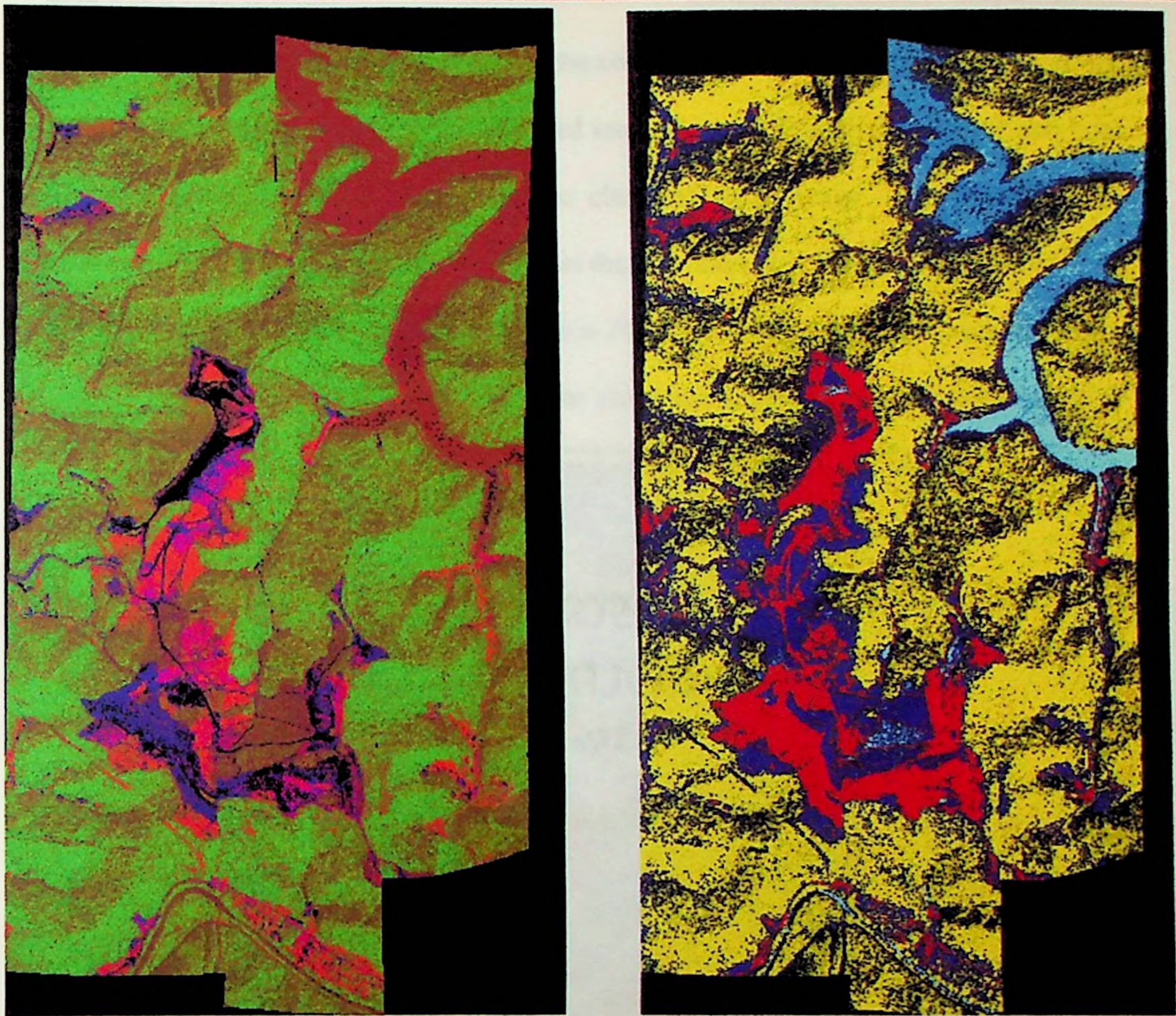

a. b.

Figure 3.12. Side by side comparison of classified PCA mosaic images. Figure a. was processes with PC 1, 2, and 3. Figure b. was processed with PC 1 and 2. Displayed in ER Mapper 6.1

PCA 3 contained little to no information with regards to sediment plume of the water, and therefore making it an unnecessary component in the classification thus reducing the dataset.

3.45 PCA WITH DEM

To incorporate the DEM data into the combination PCA 1 and 2 image and check for improvements in clustering, a classified image was performed. The water and coal already displayed good separation in the classified PCA image. The improvement between urban and surface mine was within the combination PC 1 and 2 image (Fig 3.12 b.). The image created by the combination PC 1 and 2 with the DEM was shown in figure (3.13). Note the separation within the water was gone. This image included a high

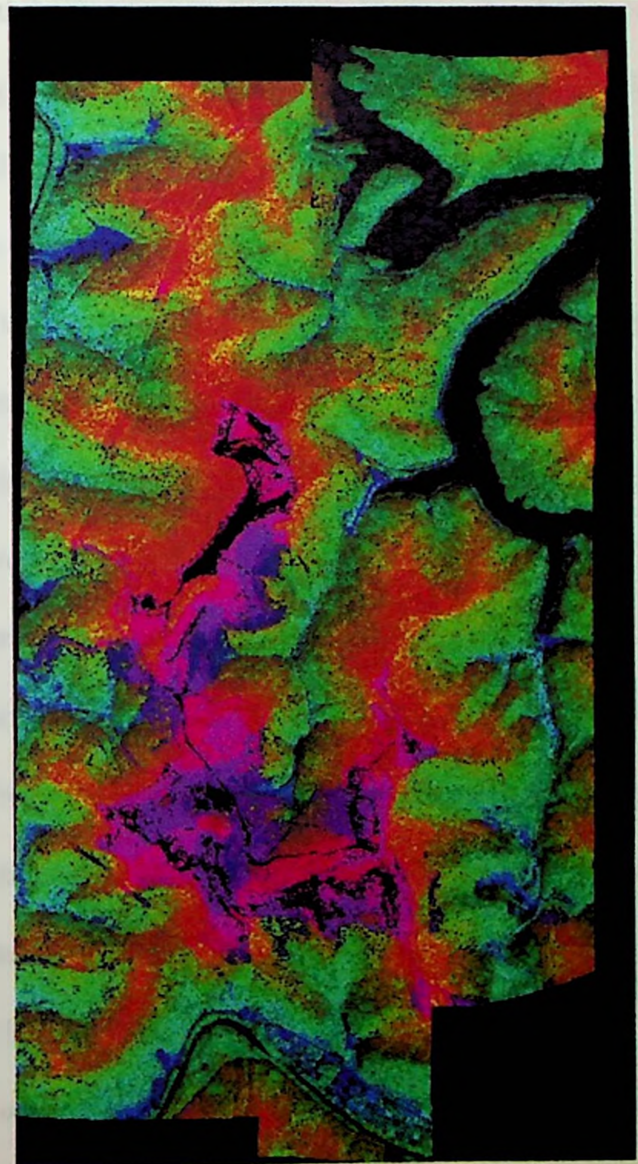

Figure 3.13. Classified image with combination PC 1 and 2 with the DEM in ER Mapper 6.1.

percentage of null values, which appeared black. This occurred when a pixel was not placed into a cluster thereby decreased the desired percentage unchanged on the ISOCLASS module. This caused excessive iterations that greatly increased processing time. The DEM was weighted too heavily within the PC combination of 1 and 2. The combination and elimination of data from the dataset bands, going from 6 bands of spectral information to 2 bands, proved to place too much loading importance on the DEM data. This decreased weighted feature extraction capabilities within the combination PC 1 and 2 imagery. In Figure 3.13 the red coloration was due to elevation variability alone and presented a false spectral feature on the classified image.

3.46 FIELD MEASUREMENTS

Field samples were taken from selected locations of Dewey Lake. Samples taken back to Marshall University were test for dissolved metals (See Appendix 1). There was a total of 36 elements tested, 5 of which are commonly associated with acid mine drainage. These included aluminum, cadmium, copper, iron, and zinc, none of which showed increased levels due to surface mining activity. However, 3 elements, calcium, magnesium and potassium, had elevated concentrations as a result of the mining activity. The high concentrations of calcium and magnesium helped explain the high pH measurement taken from Dewey Lake. The activity of these metals was directly related to the pH of the water. For example, iron only goes into solution at low pH levels. Therefore, within Dewey Lake metals associated with acid mine were not expected drainage because the lower pH level was not present.

The samples were tested for suspended sediment by pouring the water into glass beakers and visually examining for clarity. There was a pronounced colorshift within the sample collected outside of the water classified as carrying the suspended sediment load. This sample was crystal clear upon visual examination. Where as the samples collected within the area classified as suspended sediment load was cloudy indicating higher levels of sediment in suspension.

Chapter Four

CONCLUSION AND FUTURE TRENDS

The present work demonstrated the utility of digital remotely sensed data for geobiophysical modeling the environmental impacts of surface coal mining in the Appalachian coalfields. The study was carried out using various digitally processed imagery, histogram equalization, 3-D visualization, and unsupervised classification techniques for feature extraction in pattern recognition and geobiophysical modeling.

From the six bands available for processing the band selection 5, 3, and 2 were found most useful for delineating and differentiating several environmental factors, including coal, water bodies, barren lands, sediment load, and vegetation. On the other hand, bands 4, 3, and 2 were suitable for delineating and differentiating the different vegetation types (e.g., deciduous forests, conifer forest, and stressed vegetation).

Classification was improved by incorporating DEM data into the statistics calculated within ER Mapper as a separate band of information for feature extraction. This was most effective for areas of similar spectral signature but with a large separation in elevations. There were four areas improved in feature extraction classification with the inclusion of DEM data. The classes improved were coal, water, urban, and barren soil.

Principal component analysis was useful in reducing the amount of data and discrimination of features in extraction for pattern recognition. This data reduction occurred without losing valuable information for feature extraction. The inclusion of DEM data with the PCA's demonstrated a need for a weighting factor for the DEM data. The decrease in the amount of redundant information demonstrated an increase in the DEMs weighting on the classification. This influence was extremely strong which deterred classification and showed contour zoning around elevation, this proved to be a negative influence on the classification.

PC 1 and 2 proved better in clustering the images than did PC 1, 2, and 3. The explanation lies within the data, because PC 3 included most of the periodicity and noise, thereby providing much unwanted information. This caused a high percentage of null cells not used in the classification. A desired level of null cell values would be in the range of 5% or less. With the inclusion of PC 3, this level was in the range of 40 %.

The classification worked best when all bands were included in the calculations as compared with band combination 6, 5, and 2. The latter were chosen statistically to provide the least amount of redundant information and demonstrated visually the best combination to separate coal from water. This was a three band classified image which improved processing time by reducing file size, but at the same time reduced the accuracy substantially in the classification. Whereas the PCA combination 1 and 2 reduced file size more so than even the three band combination, but it did not seem to diminish the quality of the classified image.

Several environmental indicators associated with surface coal mining were evaluated. These included suspended sediment load, acid mine drainage, stressed vegetation and land degradation, due to surface mining activity. Only two indicators were found to be affecting Dewey Lake, a heavy suspended sediment load and land degradation. Although not all were found within the study area, the techniques developed here were valid for locating all four environmental indicators. These techniques can be applied for a quick evaluation of mining activity within the Appalachian mountains.

A more detailed model could be made to research the environmental impact of the mining operations. This would include additional physical parameters to the input data for geobiophysical modeling. Some of these would include temperature, moisture, and percentage cloud cover to develop a short-term trend evapotranspiration suitability index. To develop a long term trend of climate suitability, data included would be relative humidy, temperature, precipitation, wind velocity, and rain location. Adding data such as vegetation, crops, and wildlife habitat would create a vegetation index.

References

ALEXANDER, S. S., Dien, J., and Gold, D. P., 1973, The use of ERTS-1 MSS data for mapping strip mines and acid mine drainage in Pennsylvania. *Proceeding of the Symposium on Significant Results obtained from the Earth Resources Technology Satellite-1.* Maryland, U.S.A., 5-9 March 1973 (Washington, D.C.: National Aeronautics and Space Administration), Volume I, section 1, pp. 569-575.

ALFOLDI, T. T., 1982, Remote sensing for water quality monitoring. *In Remote Sensing for Resource Management*, edited by C. J. Johannesen and J. L. Sanders (Ankeny , Iowa: Soil Conservation Society of America), pp. 317-328.

ANDERSON, J. R., 1971, Land-use classification schemes. *Photogrammetric Engineering and Remote Sensing*, 37, 379-387.

ANDERSON, A. T., and SCHUBERT, J., 1976, ERTS-1 data applied to strip mining. *Photogrammetric Engineering and Remote Sensing*, 42, 211-219.

ANDERSON, A. T., SCHULTZ, D., BUCHMAN, N., and NOCK, H, M., 1977, Landsat imagery for surface mine inventory. *Photogrammetric Engineering and Remote Sensing, 43, 1027-1036.*

ANDERSON, J. E., and TANNER, C, E., 1978 Remote monitoring of coal strip mine rehabilitaion. U.*S. Environmental Protection Agency, Environmental Monitoring and Support Laboratory*, Las Vegas, Nevada. Report No. EPA-600/7-78-149 (PB-286 647).

BARR, D. J., 1981, Landsat applications to surface mining. *Proceedings of the International Conference on Computing in Civil Engineering held at New York,* 12-14 May 1981 (New York: American Society of Civil Engineers), pp. 384-396.

BAUER, H. J., 1973, Ecological aerial photo interpretation for revegetation in the Cologne lignite district. Ecology and reclamation of devastated land. *Proceedings of a Symposium on the Ecology and Revegetation of Drastically Disturbed Areas. University Park, Pennsylvania, 3-16 August 1969*, edited by R.J. Hutnik and G. Davis (New York: Gordon and Breach, Scientific Publications), 2, pp. 469-476.

BLOEMER, H. H. L., BRUMFIELD, J.O., OBERLY, R. E., AND SANDERSON, D. 1996, A Comparative Analysis of Very High Resolution Multispectral and TM Data in Feature Extraction for the Appalachian Mountains. *Proceedings of the 4th International Symposium on High Mountain Remote Sensing Cartography,* August 1996. Sweden.

BLOEMER, H. H. L., BRUMFIELD, J.O., OBERLY, R. E., AND SANDERSON, D.

1996, Resolution multi spectral multistage sensor data in feature extraction for the Appalachian mountains. *Proceedings of the 4th International Symposium on High Mountain Remote Sensing Cartography,* August 1996. Sweden.

BRUMBAUGH, J. E., 1979, Strip mine reclamation and remote sensing technology. *Mining Congress Journal*, 65, 57-61.

BRUMFIELD, J. O., 1990. Geobiophysical Modeling systems. *Ph.D. Dissertation*, The Union Institute Graduate School, Cincinnati, Ohio.

BRUMFIELD J. O., BLODGET H. W., MARCELL R. F., and WITT R. G., 1983. Comparative Techniques used to evaluate Thermatic Mapper Data for Land Cover Classification in Logan County, West Virginia. *Proceedings of the Landsat-4 Science Characterization Early Results Symposium,* 22-24 February 1983 Greenbelt, Maryland. Report No. NASA CP-2355, pp. 403-414.

CARREL, J. E., JOHANNSEN, T, W., BARNEY, T. W., and McFARLAND, W., 1978, Remote measurements of vegetative cover in surface mines. *Proceedings of the Twelfth International Symposium on Remote Sensing of the Environment. 20-26 April, 1978 Centre for Remote Sensing Information and Analysis, Environmental Research Institute of Michigan* (Ann Arbor, Michigan: E.R.I.M.), III, pp. 1653-1664.

CARR, J. R., GLASS, C. E., and SCHOWENGERDT, R. A., 1983 Signature extension versus retraining for multispectral classification of surface mines in arid regions. *Photogrammetric Engineering and Remote Sensing*, 49, 1193-1199.

CHASE, P. E., and PETTYJOHN, W., 1973, ERTS-1 investigation of ecological effects of strip mining in eastern Ohio. *Proceedings of the Symposium on Significant Results obtained from the Earth Resources Technology Satellite-I Maryland, U.S.A., 5-9 March 1973* (Washington D.C.: National Aeronautics and Space Administration), I, pp. 561-568.

COLLINS, G. W., FLACH, D., and McGUIRE, J., 1991, Monitoring environmental quality: derelict and degraded land survey. *Proceedings of the Conference on Remote Sensing of the Environment: Raising Awareness, held at Birmingham on 30 October 1991* (Middlesex, London: Blenhein Online), pp. 95-106.

GILBERTSON, B. P., 1973, Monitoring vegetation cover on mine dumps with ERTS-1 imagery: some initial results. *Proceedings of the Symposium on Significant Results obtained from the Earth Resources Technology Satellite-I. Maryland, U.S.A., 5-9 March 1973* (Washington, D.C.: National Aeronautics and Space Administration), 1, pp. 577-584.

GREEN, J. E., and BUSCHUR, J. P., 1980, A cost analysis of aerial photographic and satellite imagery for monitoring mined land reclamation. *Proceedings of the 1982 Symposium on Surface Mining Hydrology, Sedimentology, and Reclamation, edited by D. H. Graves, 1-5 December 1980,* Lexington, Kentucky (Lexington, Kentucky: University of Kentucky, College of Engineering) Report No. UKY BU123. Pp. 137-140.

HALVERSON, H. G., 1988, High altitude photography to evaluate coal0-mine reclamation. *Proceedings of the Second Forest Service Remote Sensing Applications Conference Slidell, Louisiana and NSTL Mississippi held on 11-15 April 1988* (Virginia: American Society for Photogrammetry and Remote Sensing), pp. 360-365.

HARDING, A. E., 1988, Monitoring Surface Mineral Workings Using TM and SPOT. *Proceedings of IGARSS'88 Symposium held at Edinburgh, Scotland between 13-16 September 1988* (Paris: European Space Agency), pp. 1671-1676.

IRONS, J. R., LACHHOWSKI, H., and PETERSON, C., 1980, Remote Sensing of surface mines: a comparative study of sensor system. *Proceedings of the 14th Symposium on Remote Sensing of the Environment held at San Jose, Costa Rica, April 1980.* (Ann Arbor, Michigan: Environmental Research Institute of Michigan), pp. 1041-1053.

JAHNE, B., 1991, *Digital Image Processing ; Concepts, Algorithms, and Scientific Applications.* New York: Springer-Verlag, pp. 383.

JAQUES, D., 1977, The capabilities of high-flight aerial photography and Landsat Multispectral imagery for monitoring coal reclamation activity. *Proceedings of the Coal Industry Reclamation Symposium, Banff, Alberta, 13-16 February 1977* (Calgary, Alberta: Coal Association of Canada), pp. 17-26.

JENSON, J. R., 1986, *Introductory Digital Image Processing: A Remote Sensing Perspective.* (Englewood Cliffs, N.J: Prentice-Hall), pp. 254-271.

JENSON, J. R., NARUMALANI, S., WEATHERBEE, O., and MACKEY, H. E., 1993, Measurement of Seasonal and Yearly Cattail and Waterlily Distribution Using Remote Sensing and GIS Techniques, *Photogrammetric Engineering And Remote Sensing*, 59, pp. 519-525.

JOHANNSEN, C. J., BARNEY, T. W., COBLE, A. D., CARREL, J. E., McFARLAND, W., AND BARR, D. J., 1979, Characterization of vegetation and drainage in strip mined land utilizing remote sensing techniques. *U.S. Environmental Protection Agency, Industrial Environmental Research Laboratory, Cincinnati*, Ohio. Report No. EPA-600/7-79-194. (PB80-100464).

KENNY, J. F., and McCAULEY, R., 1982, Remote sensing investigations in the coal fields of southern Kansas. *Remote Sensing for Resource Management, edited by C. J. Johannsen and J. L.Sanders* (7515 N. E. Ankeny Road: Soil Conservation Society of America), pp. 338-346.

KIRBY, C. L., 1974, Remote monitoring of environment change (summary). *Proceedings of Workshop on Reclamation of Disturbed Lands in Alberta. Edmonton, Alberta, 27-28 March 1974,* edited by D. Hocking and W. R. MacDonald. Alberta Department of Environment, Research Secretariat, Edmonton, Alberta and Canada Department of Environment, Canadian Forestry Service, North Forest Research Centre, Edmonton, Alberta. Information report No. NOR-X-116, pp. 13-14.

LATHROP, R. G., and LILLESAND, T. M., 1986, Utility of Thematic Mapper data to assess water quality in Southern Green Bay and West-Central Lake Michigan. *Photogrammetric Engineering and Remote Sensing*, 52, pp. 671-680.

LATHROP, R. G., and LILLESAND, T. M., 1988, Utility of SPOT-1 data to asses water quality in Southern Green Bay, Lake Michigan. *Technical Papers ACSM-ASPRS Annual Convention, St. Louis, 13-18 March 1988* (Falls Church Virginia: American Congress on Surveying and Mapping and American Society for Photogrammetry and Remote Sensing), 4, pp. 102-111.

LEGG, C.A., 1986, Monitoring of open cast coal mining and reclamation works in the United Kingdom using MSS and TM Imagery. *Proceedings of the 20th International Symposium on Remote Sensing of Environment* (Ann Arbor: Environmental Research Institute of Michigan), 2, pp. 931-941.

LILLESAND, T. M., LATHROP, R. G., and VANDE CASTLE, J. R., 1987, Toward an integrated system for satellite remote sensing of water quality in the Great Lakes. *Proceedings of the Fall ASPRS Meeting, Reno NV* (Virginia: American Society for Photgrammetry and Remote Sensing), pp. 342-347.

MROCZYNSKI, R. P., and WIESMILLER, R. A., 1982, Aerial photography: a tool for strip mine reclamation. *Remote Sensing for Resource Management*, edited by C. J. Johannsen and J.L. Sanders (7515 N.E. Ankeny Road, Ankeny, Iowa: Soil Conservation Society of America), pp. 331-337.

MULARZ, S. C., 1979, Reclamation problems in the Upper Silesia Mining District, Poland. *Ecology and Coal Resource Development-Proceedings of the International Congress for Energy and the Ecosystem. Grand Forks, North Dakota, 12-16 June, 1978*, edited by M. K. Wali (New York: Pergamon Press), pp. 480-489.

OBERG, M., LINDELL, T., NISELL, J., and SAARE, L., 1992, Extraction of information form satellite imagery to a GIS for environmental monitoring of the mining areas in northeastern Estonia. *Proceeding of the Third European*

Conference and Exhibition on Geographical Information Systems, Munich, Germany, 23-26 March 1992, edited by J. Harts, H. Ottens and H. Scholten (Amsterdam, Netherlands: EGIS Foundation), II, pp. 1365-1372.

PARKS, N. F., PETERSON, G. W., and BAUMER, G. M., 1987, High resolution remote sensing of spatially and spectrally complex coal surface mines of Central Pennsylvania: a comparison between SPOT, MSS and Landsat-5 TM. *Photogrammetric Engineering and Remote Sensing*, 53, 415-420.

REPIC, R. L., LEE, J. K., and MAUSEL, P. W., 1991, An analysis of selected water parameters in surface coal mines using multispectral videography. *Photogrammetric Engineering and Remote Sensing*, 57, 1589-1596.

ROGERS, R. H., and PETTYJOHN, W. A., 1975, Determining utility of ERTS-1 to detect and monitor area strip mining and reclamation. *National Aeronautics and Space Administration, Goddard Space Flight Centre, Greenbelt, Maryland,* Contract NAS5-21762, February 1975.

SOLOMON, J. L., MILLER, W. F., and QUATTROCHI, D. A., 1979, Development of a tree classifier for discrimination of surface mine activity from Landsat digital data. *Proceedings of the American Society of Photogrammetry 45th Annual Meeting held at Washington D.C. on 18-24 March 1979* (Falls Church, Virginia: American Society of Photogrammetry), II, pp. 607-613.

SPISZ, E. W., 1978, Application of multispectral scanner data to the study of an abandoned surface coal mine. *U.S. National Aeronautics and Space Administration, Lewis Research Centre, Cleveland, Ohio*. Technical Memorandum 78912.

U.S. ENIVIRONMENTAL PROTECTION AGENCY (EPA), 1975, An application of ERTS technology to the evaluation of coal strip mining reclamation in the Northern Great Plains. *Final Report, U.S. Environmental Protection Agency, National Field Investigations Center, Denver, Colorado.* Report No. EPA-330/3-75-001.

WIER, C. W., WOBBLER, F. J., ORVILLE, R. R., and AMATO, R.V., 1973, Fracture mapping and strip mine inventory in the midwest by using ERTS-1 Imagery. *Proceedings of the Symposium on significant results obtained from the Earth Resources Technology Satellite-I. Maryland, U.S.A. 5-9 March 1973* (Washington D.C.: National Aeronautics and Space Administration), pp. 553-560.

SOFTWATER AND INTERNET REFERENCE

ARCVIEW. 1991-1999, Environmental Systems Research Institute (ESRI), Redlands, CA.

ER MAPPER. 1998-2000, Earth Resource Mapping, Perth, Australia.

KENTUCKY ATLAS AND GAZZETTE. 2000, http://www.uky.edu/KentuckyAtlas/kentucky-atlasp.html. 2 July.

Geocommunity. 2000, www.geocomm.com. 21 March.

Elevation Program. 2000, http://rmmcweb.cr.usgs.gov/elevation/. 21 March.

Airborne Multispectral Digital Camera. 2000, http://www.sensystech.com/Imaging/AMDC.html. 21 March.

APPENDIX

Sample	Sample 1	Location: close to dam
Element	Concentration	ppm
Ag	0.0074	ppm
Ti	-0.0754	ppm
Pd	0.0240	ppm
Zr	-0.0565	ppm
Y	-.00116	ppm
As	0.6089	ppm
Sn	0.2822	ppm
Se	-0.5534	ppm
Ca	-1.348	ppm
Al	0.2234	ppm
Mo	0.2418	ppm
Sr	-0.3558	ppm
La	-0.0142	ppm
Ba	0.0843	ppm
Co	0.0567	ppm
Ni	-0.0563	ppm
Si	4.169	ppm
Sb	16.35	ppm
Mn	-0.000	ppm
Fe	-0.001	ppm
Pt	-0.0521	ppm
Au	-0.0113	ppm
Cr	-.0016	ppm
Mg	24.14	ppm
V	0.005	ppm
Na	35.89	ppm
Be	-0.0261	ppm
B	2.636	ppm
Ca	26.88	ppm
Zn	0.1452	ppm
Cd	-0.0060	ppm
P	-0.7617	ppm
Cu	0.0095	ppm
Pd	0.0816	ppm
Li	0.00217	ppm
K	9.873	ppm

Sample **Sample 2** **Location: Boat ramp down from camp ground**

Element	Concentration	ppm
Ag	-0.0144	ppm
Ti	-0.08144	ppm
Pd	0.02755	ppm
Zr	0.01792	ppm
Y	-.00113	ppm
As	-0.08269	ppm
Sn	0.6575	ppm
Se	0.4733	ppm
Ca	52.01	ppm
Al	0.01506	ppm
Mo	-.00890	ppm
Sr	0.9458	ppm
La	-0.0149	ppm
Ba	0.09013	ppm
Co	-0.0029	ppm
Ni	-0.06157	ppm
Si	3.944	ppm
Sb	15.68	ppm
Mn	-0.000	ppm
Fe	-0.0058	ppm
Pt	-0.0515	ppm
Au	-0.0029	ppm
Cr	-.00367	ppm
Mg	26.14	ppm
V	0.01362	ppm
Na	41.20	ppm
Be	-0.0255	ppm
B	2.248	ppm
Ca	32.63	ppm
Zn	0.004083	ppm
Cd	-0.08814	ppm
P	-1.363	ppm
Cu	0.00408	ppm
Pd	0.0816	ppm
Li	0.002	ppm
K	11.44	ppm

Sample	Sample 3		Location: Sediment pond
Element	Concentration	ppm	
Ag	0.016	ppm	
Ti	-0.08069	ppm	
Pd	0.0049	ppm	
Zr	-0.02454	ppm	
Y	-.000660	ppm	
As	0.7386	ppm	
Sn	0.1641	ppm	
Se	1.285	ppm	
Ca	134.6	ppm	
Al	0.4964	ppm	
Mo	-0.058	ppm	
Sr	1.340	ppm	
La	-0.0138	ppm	
Ba	0.0759	ppm	
Co	0.0481	ppm	
Ni	-0.0666	ppm	
Si	2.524	ppm	
Sb	9.886	ppm	
Mn	-0.000	ppm	
Fe	-0.000	ppm	
Pt	-0.0633	ppm	
Au	-0.0166	ppm	
Cr	-.01021	ppm	
Mg	83.34	ppm	
V	0.0118	ppm	
Na	12.04	ppm	
Be	-0.02584	ppm	
B	2.280	ppm	
Ca	91.57	ppm	
Zn	-0.07	ppm	
Cd	-0.00	ppm	
P	-0.212	ppm	
Cu	0.001586	ppm	
Pd	0.6520	ppm	
Li	0.001939	ppm	
K	31.30	ppm	

Sample	Sample 4		Location: close to marina
Element	Concentration	ppm	
Ag	-5.048	ppm	
Ti	-0.0778	ppm	
Pd	0.01695	ppm	
Zr	-0.039	ppm	
Y	-.0015	ppm	
As	-1.031	ppm	
Sn	0.4542	ppm	
Se	1.110	ppm	
Ca	49.50	ppm	
Al	0.2701	ppm	
Mo	-0.000	ppm	
Sr	-0.9281	ppm	
La	-0.0146	ppm	
Ba	0.0931	ppm	
Co	0.000	ppm	
Ni	-0.0596	ppm	
Si	3.889	ppm	
Sb	14.96	ppm	
Mn	-0.000	ppm	
Fe	0.010	ppm	
Pt	-0.0670	ppm	
Au	-0.02686	ppm	
Cr	0.0110	ppm	
Mg	26.88	ppm	
V	0.014	ppm	
Na	42.56	ppm	
Be	-0.0255	ppm	
B	2.065	ppm	
Ca	29.86	ppm	
Zn	0.09677	ppm	
Cd	0.1366	ppm	
P	-0.8540	ppm	
Cu	0.0040	ppm	
Pd	0.1745	ppm	
Li	0.0011	ppm	
K	13.72	ppm	

Sample	Sample 5	Location: Stratton Branch
Element	Concentration	ppm
Ag	-0.0514	ppm
Ti	-0.0771	ppm
Pd	0.0027	ppm
Zr	-0.02613	ppm
Y	-.001549	ppm
As	0.0759	ppm
Sn	0.07703	ppm
Se	-0.6854	ppm
Ca	48.96	ppm
Al	0.00710	ppm
Mo	-0.2110	ppm
Sr	0.9510	ppm
La	-0.0141	ppm
Ba	0.0900	ppm
Co	0.01313	ppm
Ni	-0.05967	ppm
Si	3.805	ppm
Sb	14.97	ppm
Mn	-0.000	ppm
Fe	-0.001	ppm
Pt	-0.0693	ppm
Au	0.02887	ppm
Cr	.00013	ppm
Mg	26.61	ppm
V	-0.006	ppm
Na	42.55	ppm
Be	-0.02312	ppm
B	1.892	ppm
Ca	29.66	ppm
Zn	-0.026	ppm
Cd	0.08954	ppm
P	-1.075	ppm
Cu	0.0014	ppm
Pd	0.1311	ppm
Li	-.002724	ppm
K	12.79	ppm